

**Neutronics Characteristics, Shielding System, Activation
and Environmental Aspects of ARIES-ACT-2 Power Plant**

L. El-Guebaly and L. Mynsberge

Fusion Technology Institute
University of Wisconsin
1500 Engineering Drive
Madison, WI 53706

<http://fti.nead.wisc.edu>

December 2014

UWFDM-1418

Abstract

The ARIES team has completed the detailed design of ARIES-ACT-2 with conservative physics and technology. The integration of nuclear assessments (neutronics, shielding, and activation) is an essential element to the success of a well-optimized design. High fidelity in nuclear parameters mandates performing state-of-the-art nuclear analyses. This has been achieved through coupling the CAD system directly with 3-D neutronics codes to preserve all geometrically complex design elements and speed up feedback and iterations. The neutron wall loading (NWL), tritium breeding ratio (TBR), and nuclear heating distribution are parameters that must be determined for tritium self-sustainability and adequate shielding and protection of ARIES fusion power plants. An integral approach considered the overall ARIES-ACT-2 configuration, design requirements (including tritium self-sufficiency), smart selection of low-activation material for each component, radial build optimization and definition, and environmental concerns.

ARIES-ACT-2 generates sizable amount of mildly radioactive materials. Disposing such a radwaste in geologic repositories is not a viable option. Alternatively, the recycling and clearance approaches were examined using rigorous activation analyses for all components comprising the fusion power core and biological shield.

I. Introduction

The ARIES team [1] has developed four power plants that are designed with a range of aggressive and conservative tokamaks (ACT) [2]. The four ARIES-ACT designs (refer to Fig. 1) proceeded interactively while the systems code determined the reference parameters through varying the physics and engineering parameters to produce an economic optimum for each design:

- Aggressive physics with SiC-based blanket (ARIES-ACT-1)
- Conservative physics with ferritic steel-based blanket (ARIES-ACT-2).
- Aggressive physics with ferritic steel-based blanket (ARIES-ACT-3)
- Conservative physics with SiC-based blanket (ARIES-ACT-4).

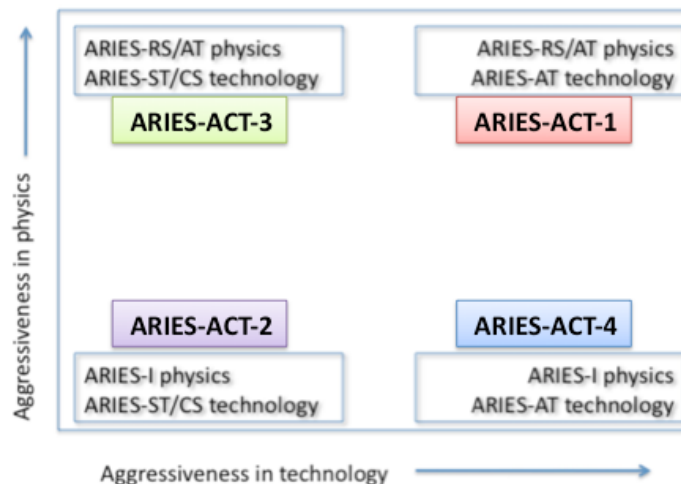


Fig. 1. Four-corner designs of ARIES-ACT power plants.

One of the main objectives of the nuclear assessment is the extensive use of 3-D analyses to guarantee the accuracy of the overall TBR with high fidelity, the evaluation of the neutron wall loading (NWL) distribution, the definition of the radial/vertical builds that satisfy the shielding, breeding, and other design requirements, the determination of the radiation damage profile particularly behind assembly gaps, the assessment of nuclear heat loads to all components, and the evaluation of the activation level and environmental impact. Such nuclear parameters are all essential elements to characterize the nuclear environment for ARIES-ACT-2 – the last power plant design in the ARIES (Advanced Research, Innovation, and Evaluation Study) series.

An integral scheme that considered the overall configuration, design requirements, low-activation materials choice, nuclear assessments, structural integrity of all components, and safety considerations was deemed necessary to deliver an optimal design. The integration of the nuclear assessments into the design began by extensive 3-D analyses to define the dimensions of inboard and outboard blankets that satisfy the breeding requirement. Then, the NWL is found for the actual 3-D configuration of FW and divertor. Such a NWL profile provides the information needed to define the radial and vertical builds based on peak values at inboard (IB) midplane, divertor dome, and outboard (OB) midplane. The shielding design then proceeds to size and optimize the shielding components taking into consideration the effectiveness of the preferred shielding materials, their activation characteristics, and safety impact. Once the radial/vertical builds are defined with other design inputs, the integration process begins using the CAD system where more complexities in the geometry can be added. Then, detailed economic and safety assessments follow with close interactions with neutronics.

ARIES-ACT-2 utilizes the dual cooled LiPb (DCLL) blanket with helium-cooled reduced activation ferritic/martensitic (RAFM) steel structure, LiPb breeder and SiC flow channel inserts (FCI), much like the ARIES-ST and ARIES-CS designs [4,5,6,7] with many commonalities and differences. As in ARIES-ST, the LiPb allows not only breeding, but also self-cooling of the blanket. The He-cooled F82H RAFM steel first wall (FW) serves to protect the blanket from heat and neutron fluxes from the plasma. In the ARIES-ACT-2 design, shown in Fig. 2, the structural ring (SR) serves as the high-temperature (HT) shield and is cooled with helium. The W-based divertor is also cooled with helium. Two separate components exist outside the SR: a thin He-cooled vacuum vessel (VV) followed by a water-cooled low-temperature (LT) shield. Note that the ARIES-ACT-2 major radius and overall machine size are driven by the peak heat flux at the divertor, rather than by the inboard radial standoff as in all previous ARIES tokamaks. This shift in design philosophy negated the need for compact, highly efficient inboard shielding components with WC filler. In other words, the ARIES-ACT-2 inboard standoff does not have a significant impact on the overall machine size and economics.

The nuclear parameters reported herein belong to the final design with a major radius of 9.75 m, minor radius is 2.44 m, plasma surface area of 1440.5 m², fusion power of 2637.5 MW, and net electric power of 1000 MW. The nuclear analysis covers three closely related tasks: neutronics, shielding, and activation. The breakdown of each subtask includes:

Neutronics:

- Neutron wall loading distribution: peak and average values
- Tritium breeding ratio (TBR) for T-self sufficiency
- Radial and poloidal nuclear heating distribution (for thermal hydraulic analysis)
- Nuclear energy multiplication (for power balance)
- Energy split between He and LiPb coolants
- Radiation damage to structural materials (dpa, He production, etc.)

- Service lifetimes of all components based on neutron dose (for replacement frequency and cost).

Shielding:

- Shielding of permanent components (for protection against radiation)
- Radial and vertical build definition (for physics code, CAD drawings, and systems code analysis)
- Neutron streaming through assembly gaps and penetrations (for radiation damage profile and biodose around torus)
- Bioshield specifications.

Activation:

- Radioactive product inventory (for safety, environmental, and licensing assessments)
- Environmental impact of fusion: radwaste classification, recycling, clearance
- Decay heat (for thermal response of components during LOCA/LOFA events)
- Biological dose (for maintenance crew, workers and public protection).

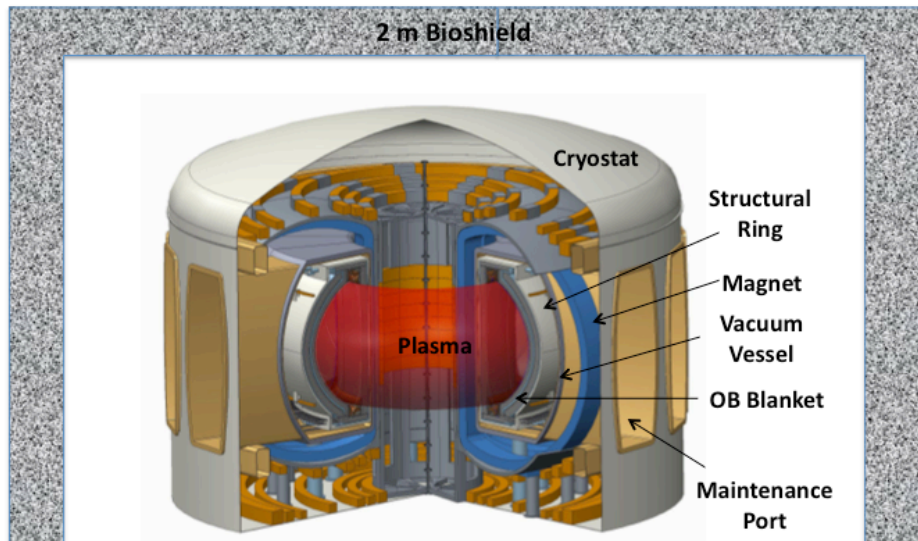


Fig. 2. Isometric view of ARIES-ACT-2 showing FPC components surrounded with cryostat and 2 m thick biological shield.

Beginning in the mid 2000 and continuing to the present, high fidelity in nuclear results mandated performing state-of-the-art 3-D nuclear analyses for several fusion designs [7-12]. As will be discussed shortly, this has been achieved for ARIES-ACT-2 through coupling the CAD system directly with the 3-D MCNP code [13], using DAGMC [14] – a newly developed code by the University of Wisconsin-Madison. Such a coupling (based on direct tracking in CAD using the MCNP physics) preserves all geometrically complex design elements and speeds up feedback and iterations to quickly converge on an acceptable configuration that satisfies the design goal, mission, and requirements. The following sections present neutronics, shielding, and activation results for selected topics addressed during the course of this study.

II. 3-D Model and Codes

A suite of computer codes and nuclear data library were utilized to perform the neutronic analysis for ARIES-ACT-2: CUBIT [15], MCNP5 [13], DAGMC [14], and FENDL-3 data library [16]. CUBIT builds the 3-D model to be used by DAGMC to perform the Monte Carlo radiation transport directly onto the computer-aided design (CAD) model, which is incredibly useful for complex geometries. The DAGMC (Directly Accelerated Geometry Monte Carlo) code is a software tool developed by the Computational Nuclear Engineering Research Group (CNERG) of the University of Wisconsin-Madison to perform Monte Carlo radiation transport on complex 3-D geometries created by solid modeling software [10]. DAGMC converts any complex 3-D geometry into a faceted geometry of tetrahedrons and couples it to the radiation transport code MCNP5 and its FENDL-2.1 continuous pointwise cross section data library.

ARIES-ACT-2 has 16 toroidal modules separated toroidally by 2 cm wide assembly gaps. Each of the 16 modules spans a 22.5° toroidal angle. The upper half of an 11.25° wedge of the tokamak was modeled for the 3-D TBR and nuclear heating analyses, representing one quarter of module or 1/64th of the entire tokamak. We made use of three reflecting boundaries placed at both sides of the 11.25° wedge and at the midplane to make the 1/64 neutronics model equivalent to the full toroidal geometry.

Three nested regions within the plasma boundary with 63.0%, 32.5%, and 4.5% intensities present the neutron source distribution. The magnetic axis is shifted outward by ~ 30 cm from the major radius. When we compared the actual neutron source distribution on R-Z grid from plasma physics simulations by PPPL, the three-region presentation of the neutron source proved to capture almost all effects of the actual source and yielded comparable NWL and TBR results. The 3-D results reported herein exhibit acceptable statistical errors ($\ll 1\%$ for the overall TBR, $< 1\%$ for the NWL, $< 5\%$ for the nuclear heating of front components, and $< 8\%$ for the nuclear heating of back components)

III. Tritium Breeding Assessment

The ability of the DCLL blanket to provide tritium self-sufficiency is among the most important issues that we investigated in detail for ARIES-ACT-2 to pinpoint the design elements that impact the breeding. The main goal of this assessment is to identify the exact damaging/enhancing conditions to the TBR caused by the internal components of the blanket as well as the external, essential parts of the tokamak. To overcome the challenges of dealing with tritium-related uncertainties in several subsystems, we suggest operating all LiPb employing designs with ^6Li enrichment $< 90\%$ and adjusting the Li enrichment online during operation to mitigate concerns about shortage or surplus of tritium.

III.A. ARIES-ACT Tritium Breeding Requirement

The four ARIES-ACT designs require the calculated TBR to be 1.05 [17]. Historically, the breeding margin (calculated TBR - 1) evolved with time [17], reaching its lowest value (0.05) for ARIES-ACT. This breeding margin can be divided into four distinct categories [18]:

- Margin that accounts for known deficiencies in nuclear data (3%)
- Margin that accounts for known deficiencies in modeling (1%)
- Margin that accounts for unknown uncertainties in design elements (0%)
- Margin that accounts for T bred in excess of T consumed in plasma (1%).

The values between parentheses indicate the expected contribution of each category to the breeding margin of ARIES-ACT-2, meaning a calculated TBR of 1.05 for the LiPb breeder. The 3% of the first margin is derived from the most recent experiment at ENEA to validate the nuclear data for the LiPb breeder [19]. The C/E is $1 \pm 5\%$ including the uncertainties in measurements. Based on an educated guess, the deficiency in the LiPb nuclear data could be around $\pm 3\%$. This value is not so critical for ARIES-ACT-2 since the design mandates the online adjustment of breeding. A few percent up or down in breeding can be recovered during operation by adjusting the ${}^6\text{Li}$ enrichment online, as discussed later in Section III.B.

As noted in detail in Section III.C, the ARIES-ACT-2 3-D TBR model includes all the engineering details of the blanket. The second margin of 1% accounts for any overlooked design element. The related third margin has been zeroed out as our 3-D model includes all structural details specified by blanket designers. If unforeseen design modifications negatively impact the TBR as the design evolves towards a mature engineering design, the online adjustment of the ${}^6\text{Li}$ enrichment will compensate the losses in breeding. The last 1% margin (~ 1.5 kg of T per full power year) accounts for the T bred in excess of T consumed in the plasma. Such an excess T is required to provide the startup inventory for a new fusion power plant, to compensate for the decay of the total T inventory, and to account for the T lost to the environment [18].

The 5% sum of the three margins derives the minimum TBR (1.05) necessary for reliable breeding in ARIES-ACT-2. Because the deficiencies in the LiPb nuclear data (3%) and modeling (1%) both tend to reduce the breeding, the Net TBR during plant operation could be as low as 1.01. Such a low Net TBR of 1.01 is practically achievable in fusion designs employing advanced physics and technology where the T fractional burnup exceeds 10%, the T inventory is minimal, and the T extraction and reprocessing system are highly reliable [18]. Note that the few percent difference between the calculated TBR and Net TBR will decrease in the future as the nuclear data evaluation improves with a dedicated R&D program.

III.B. Need for Online Adjustment of TBR

The Net TBR of 1.01 will not be verified until after DEMO operation with fully integrated blanket, T extraction, and T processing systems. A shortage of T impacts the plant operational schedule and mandates purchasing T from outside sources with uncertain pricing (\$30,000 - \$100,000 for a gram of T) while a surplus of T introduces licensing and storage problems. Thus, it is less risky to design an over-breeding blanket with the understanding that an online adjustment of the breeding level is feasible through fine-tuning of the ${}^6\text{Li}$ enrichment. It is also possible that early generations of fusion plants could require a Net TBR > 1.01 for shorter doubling time while a mature fusion system may call for $1.002 < \text{Net TBR} < 1.01$. Moreover, fusion plants may not operate in a uniform manner, generating more/less T during operation according to the need for variable doubling time, the need for higher/lower breeding over a certain time period (with the same integral amount of T over blanket lifetime), and/or the availability of T recovered from the detritiation system. Equally important for licensing considerations, fusion designs should not generate more T than needed for plasma fuelling. All these issues support the argument that an online adjustment of breeding is a must requirement for DEMO and power plants.

Historically, all LiPb-based blankets utilized 90% enriched ${}^6\text{Li}$ to maximize the breeding. Only in recent ARIES studies [7,12,17], the design point has been shifted to $< 90\%$ enrichment in order to provide an extra margin to increase the TBR online, if needed. References 18 and 20

outline two practical methods for the online adjustment of the Li enrichment of LiPb along with the pros/cons for each method and potential improvements as the breeding margin decreases with time. Note that the online adjustment of breeding is feasible for liquid breeders only and difficult to envision for ceramic breeder blankets.

III.C. 3-D TBR Model, Analysis, and Results

Besides the recent computational advancements, we developed a novel stepwise technique to fully understand the importance of each design refinement and to address several breeding-related questions that puzzled the fusion community for decades:

- How does the blanket structure (first wall, side and back walls, etc.) degrade the breeding?
- Which change to the blanket dimension, composition, and/or Li enrichment is more enhancing to the breeding?
- How does the advanced physics (that requires embedding stabilizing shells within the blanket) degrade the breeding?
- Could the required TBR be achieved in the presence of several plasma heating and current drive ports that compete for the best available space for breeding?

Past studies made several attempts to answer some questions by addressing individual issues – one at a time. However, there are still some concerns regarding the inter-dependence and synergistic impact of the various design elements on TBR and the degree of confidence in the single-effect analysis. To address these concerns collectively, we developed the stepwise approach to identify the exact cause of the degradation in TBR and examined almost all questions in an integral fashion. Note that this new approach was first applied to an interim ARIES-ACT-2 design [17] to address the questions and concerns mentioned above. Here, we reapplied the stepwise approach to the final ARIES-ACT-2 design to confirm that the most recent modifications made at the top/bottom ends of the OB blanket along with adding manifolds behind the divertor system comply with the ARIES breeding requirements (overall TBR of 1.05 with ${}^6\text{Li}$ enrichment < 90%).

Ten individual design elements contribute to the degradation in TBR. These elements belong to the internals and externals of the ARIES-ACT-2 DCLL blanket and include the FW, side/back/top/bottom walls, cooling channels, SiC FCIs, W stabilizing shells, assembly gaps, and penetrations. Special care has been taken to model all details to duplicate the exact design specifications of the blanket. The stepwise approach enabled step-by-step addition of the individual elements to the blanket envelope and recording the corresponding incremental change to the TBR. For a precise representation, the individual blanket elements were first modeled by the CAD system, and then coupled with the MCNP code through DAGMC [14]. The 3-D TBR model represents 1/64th of ARIES-ACT-1, as described in Section II. Complete heterogeneity was used for the actual LiPb breeding channels. The starting ${}^6\text{Li}$ enrichment is 90% as in ARIES-AT. At the end, the variation in TBR as a function of ${}^6\text{Li}$ enrichment was examined.

The end result is displayed in Fig. 3 for the reference LiPb eutectic that contains 15.7 at% Li and 84.3 at% Pb [21]. This bar chart represents the calculated TBR from a series of ten consecutive 3-D runs performed to illustrate the stepwise degradation in breeding by various elements of blanket internals and surroundings. The ten individual steps are discussed below along with the detailed change(s) made to the 3-D model for each step.



Fig. 3. Bar chart showing the reduction in TBR from 1.8 to 1.05 as a result of including internals and externals of ARIES-ACT-2 DCLL blanket.

Step 1: To estimate the highest achievable TBR for any LiPb system, a model of an infinite cylinder was created with 2 m LiPb with 90% ^6Li enrichment and no structure followed by 2 m thick F82H ferritic steel (FS) shield to provide the appropriate neutron reflection that enhances the breeding. The corresponding TBR for this ideal configuration is 1.79, marking the first bar in Fig. 3.

Step 2: The toroidal model was constructed using the latest ARIES-ACT-2 configuration shown in Fig. 4. In the neutronics model, the LiPb breeder is confined radially and poloidally to the space assigned for the 65 cm thick IB blanket, 100 cm thick OB blanket, and top/bottom manifolds. Surrounding components (SR, VV, LT-shield and divertor) are all added in the model. The D-shape plasma contains the three nested neutron source regions described in Section II. The two OB blanket segments are separated by a 5 cm wide gap to accommodate the W stabilizing shells. The 3-D configuration with such a limited radial and poloidal LiPb coverage dropped the TBR by $\sim 10\%$.

Step 3: There is a 2 cm wide assembly gap between adjacent modules to allow for thermal expansion, neutron-induced swelling, and radial removal of modules during maintenance. Since half of the blanket module is being considered, the gap in the 3-D model is 1 cm wide and was modeled on one side of the 11.25° wedge. The TBR degraded slightly (0.7 %) due to the addition of the gap.

Step 4: The IB and OB breeding zones are separated from the plasma region by a 3.8 cm FW composed of F82H and helium. Adding the IB and OB FWs dropped the TBR by ~9%.

Step 5: To completely enclose the IB and OB breeding blankets, side/back/top/bottom walls of various thickness and F82H and helium composition were added. The wall structures caused the TBR to drop by 2.4%.

Step 6: The IB and two OB blanket regions are segmented within the walls by adding a cooling channel structure. This structure splits the IB into 9 channels and each OB segment into 16 channels in an 11.25° wedge, as shown in Fig. 5. The number of channels has been acquired through a series of stress analyses [22]. Upon including the cooling channels, the TBR degrades by 3.7%.

Step 7: Once segmented into LiPb flow channels, a SiC FCI is added between the FS cooling channels and the flowing LiPb. This addition drops the TBR by 3.7%.

Step 8: Between the OB blanket segments, there is 4 cm thick W Vertical Stabilizing (VS) shell located between 55° and 85°, as shown in Fig. 6. There is also a VS shell behind the IB blanket that will not affect the breeding. The impact of the OB VS shell is a 3.1% drop in TBR.

Step 9: The ${}^6\text{Li}$ enrichment was varied to determine the possibility of operating ARIES-ACT-2 at lower enrichment than 90%. Figure 7 suggests an enrichment of 40% that results in ~15% reduction in TBR.

Step 10: The heating, fueling, diagnostics, and current drive penetrations occupy ~36 m² of the OB FW area, representing 4% of the OB FW area (1021 m²). Assuming a direct correspondence between the area of penetrations and the reduction in OB breeding, we would expect the TBR to drop by 2.8% due to OB penetrations, reaching 1.05.

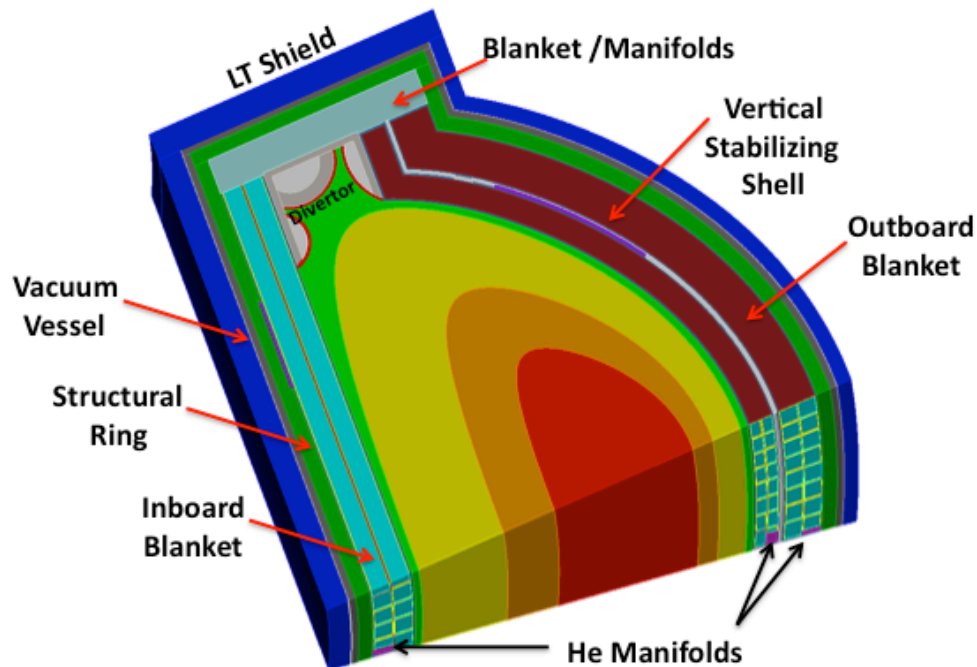


Fig. 4. Layout of IB and OB blankets and surrounding components.

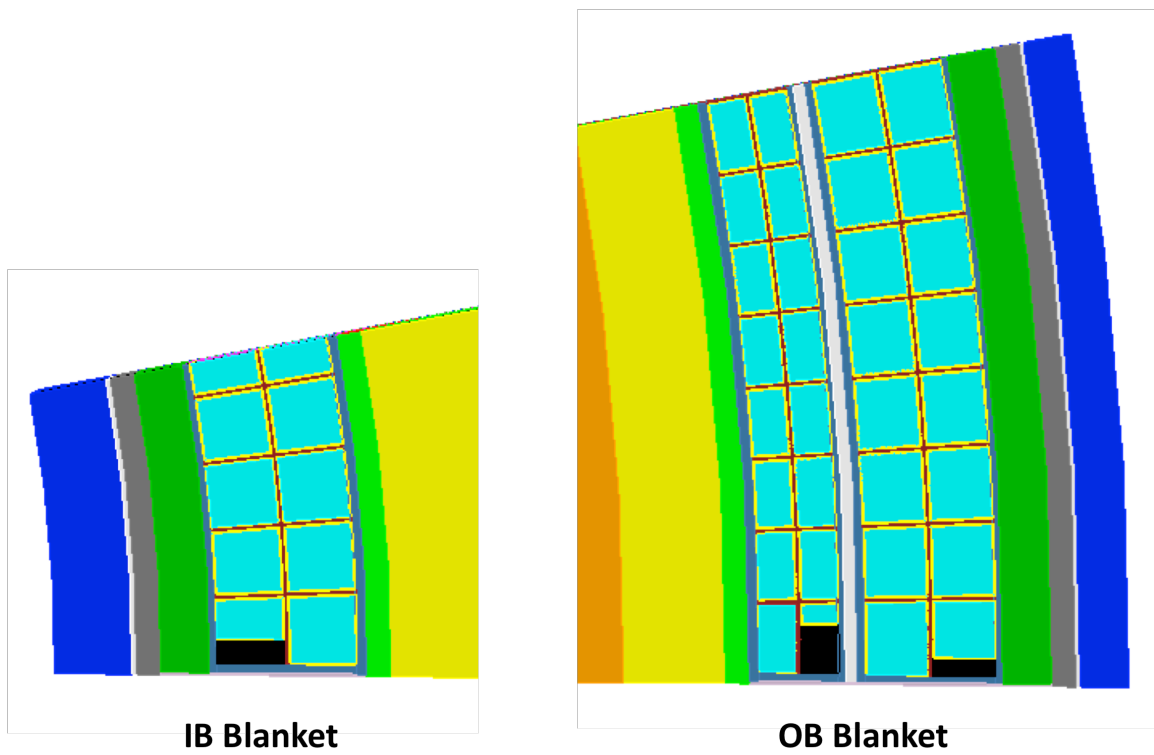


Fig. 5. Midplane cross section showing the segmentation of the breeding blankets by the cooling channels (in brown). The SiC FCI is shown in yellow.

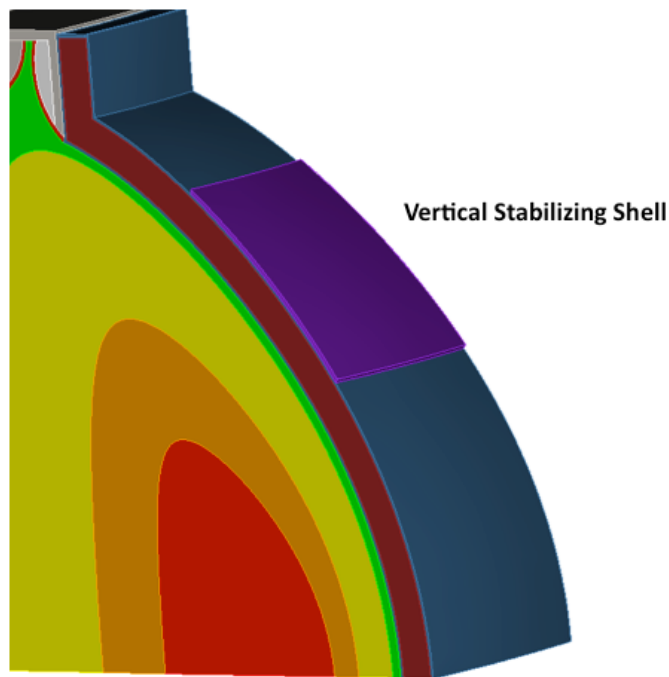


Fig. 6. Cutaway isometric showing the addition of OB W vertical stabilizing shell (in purple).

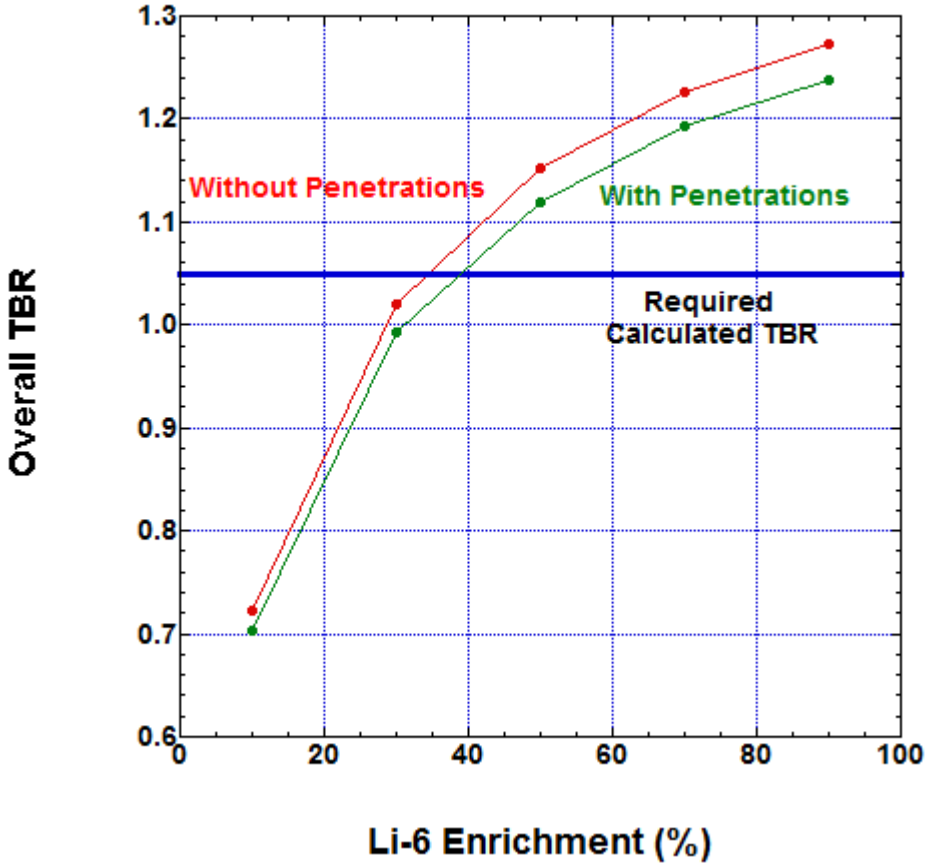


Fig. 7. Change in TBR with varying ${}^6\text{Li}$ enrichment of LiPb breeder.

III.D. Discussion and Main Findings

Our findings not only confirm the ARIES-ACT-2 blanket complies with the ARIES breeding requirements (calculated TBR of 1.05 with $< 90\%$ ${}^6\text{Li}$ enrichment), but also provide a rational basis for the damaging and enhancing changes to the breeding of several blanket design elements. The main results of this TBR analysis can be summarized in the following points:

- Limiting the blanket coverage radially and vertically has the largest single impact on TBR ($\sim 10\%$)
- The inclusion of all structural walls, cooling channels, and FCIs dropped the TBR by $\sim 18\%$.
- Stabilizing shell, penetrations, and assembly gaps have $\sim 6\%$ impact on TBR.

The OB and IB blankets contribute most of the breeding (69.3% and 27.9%, respectively), while the top/bottom blankets/manifolds behind the divertor provide the balance (2.8%). Figure 8 displays the T production within the LiPb breeder. Note that T production peaks around the midplane and fades out as one moves upward/downward and radially away from the FW. This

emphasizes the importance of the midplane for breeding and suggests keeping the OB midplane in particular free of penetrations to maximize the TBR. The figure also illustrates the inefficient divertor region for breeding and the reduction in breeding around the OB VS shell due to the strong neutron absorption by W.

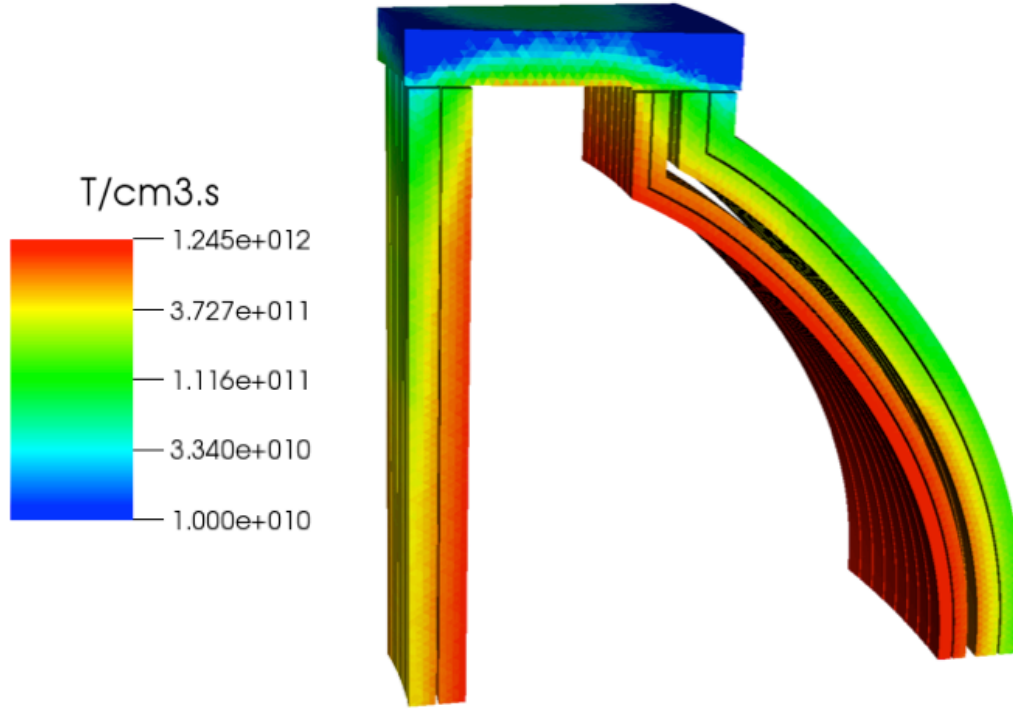


Fig. 8. Tritium production distribution within LiPb breeder.

The details of this 3-D TBR analysis are as important to many fusion scientists as is the answer to the question: will the DCLL blanket over-breed or under-breed? Because many uncertainties in the operating system govern the achievable TBR, both the achievable TBR (of 1.05) and Net TBR (of 1.01) will not be verified until after the operation of a DEMO with fully integrated blanket, T extraction system, and T processing system. Only then will the above important question have an answer. We will certainly know what to design for before building the first generation of fusion power plants. Any proposed blanket design will be redesigned accordingly. Therefore, it is necessary to have a flexible approach and any blanket design should be able to accept a few necessary changes in order to deliver a Net TBR of 1.01. For ARIES-ACT-2, the most practical solution for an over-breeding blanket (Net TBR > 1.01) is to lower the ⁶Li enrichment online, using Fig. 7 for guidance. In case of an under-breeding blanket (Net TBR < 1.01), the simplest change is to increase the ⁶Li enrichment above 40% to gain up to ~15% in TBR. If insufficient, major design changes are anticipated. These include thickening the blanket further, adding a beryllium multiplier to the blanket, and/or operating in single null mode. Clearly, some of these changes may not be feasible during operation. It is therefore less risky to design an over-breeding blanket with a feasible scheme to adjust the breeding online shortly after plant operation, as discussed earlier in Section III.B.

IV. Neutron Wall Loading Distribution

The NWL enables designers to define the radial and vertical builds, ensuring proper shielding of outer components against energetic neutrons. It is essential to evaluate the peak NWL values (for shielding and radiation damage analyses - Section V) along with other data such as average values (for the activation analysis - Section VIII).

By definition, the NWL is a fusion power normalized neutron current density at the first solid wall surrounding the plasma. It is evaluated by recording the neutron current that crosses the 3-D surfaces of first wall and divertor plates. Using CUBIT [15] to build and prepare a 3-D model of the FW and divertor in addition to DAGMC [14] to perform Monte Carlo radiation transport onto the model, neutronic simulations were performed to obtain the NWL distribution along the FW and divertor surfaces of ARIES-ACT-2. Figure 9 shows the 3-D model for this particular analysis using the three-region neutron source definition within the plasma boundary.

Results shown in Fig. 10 were obtained for the NWL distribution along the IB and OB FWs of the final ARIES-ACT-2 design (major radius of 9.75 m, minor radius of 2.44 m, and fusion power of 2637.5 MW). The peak NWL (2.2 MW/m^2) occurred at the midplane of the OB FW. As expected, the NWL decreases with the vertical distance from the midplane. Figure 11 displays the NWL distribution along each divertor plate. The radial distance for the dome is measured from the centerline of the tokamak. Note that the orientation of the divertor surface impacts the NWL, meaning a surface facing the plasma experiences a higher NWL compared to a vertical surface. Table I summarizes the NWL data obtained for the 568 m^2 IB FW, 1021 m^2 OB FW and three divertor plates.

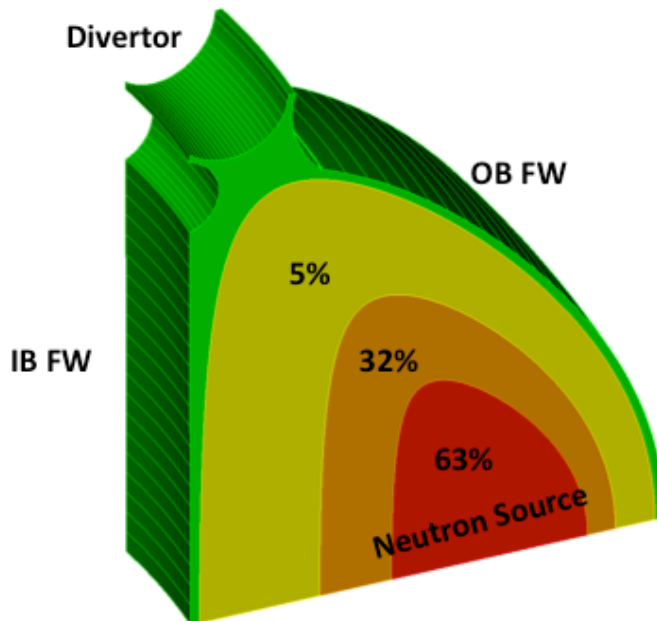


Fig. 9. 3-D ARIES-ACT-2 model used for NWL analysis. FW and divertor surfaces are segmented in order to accurately obtain the NWL at various surfaces.

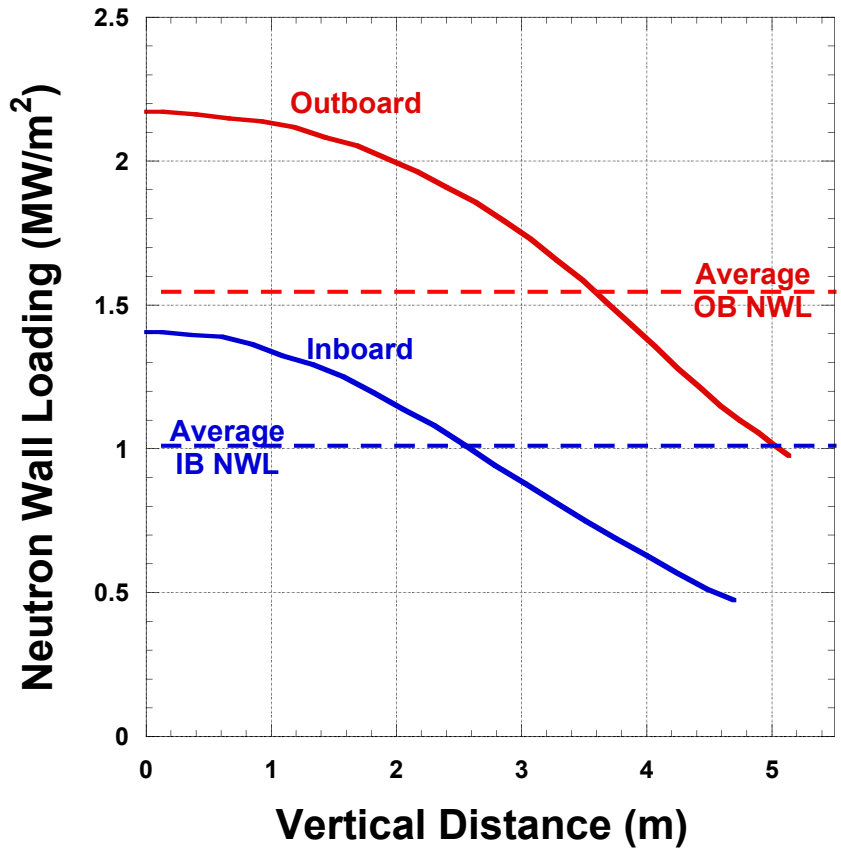


Fig. 10. Poloidal distribution of NWL at inboard and outboard FWs.

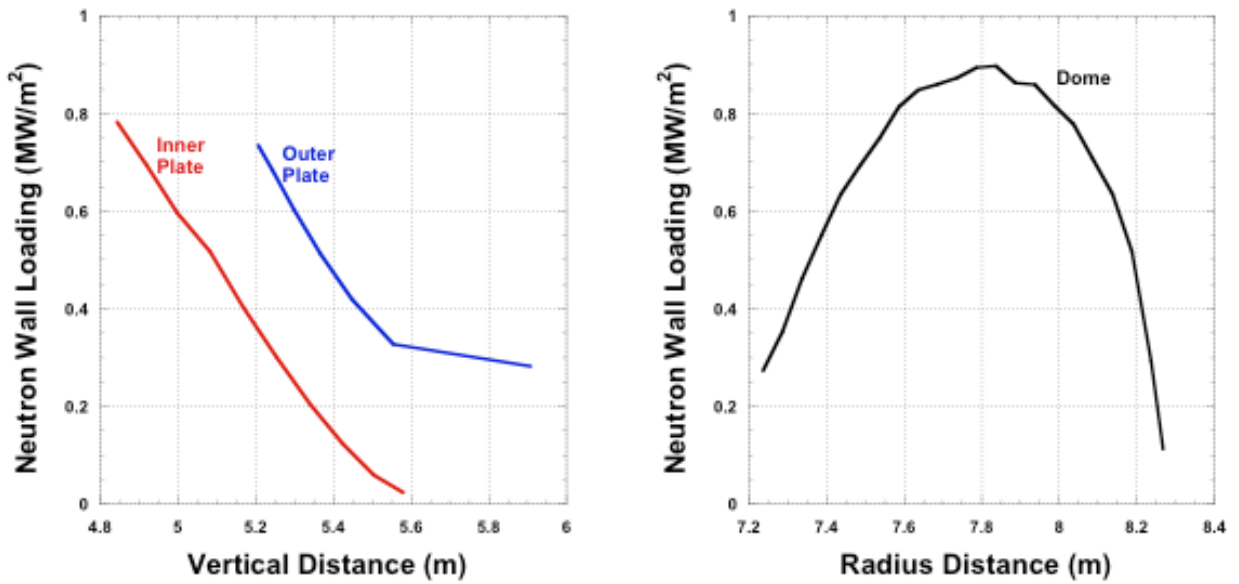


Fig. 11. NWL distribution at divertor plates.

Table I. Neutron Wall Loading Summary

| NWL (MW/m ²) | Peak | Average |
|--------------------------|------|---------|
| Machine average | | 1.45 |
| IB FW | ~1.5 | 1.0 |
| OB FW | 2.2 | 1.55 |
| Divertor | 0.9 | 0.44 |
| Inner Plate | 0.78 | 0.44 |
| Outer Plate | 0.74 | 0.30 |
| Dome | 0.90 | 0.56 |

V. Radial/Vertical Build Definition

Upon determining the blanket dimension and enrichment, the definition of radial/vertical builds proceeded with close interaction between the effectiveness of the preferred shielding materials and their activation characteristics. The He-cooled MF82H ferritic steel-based SR supports the blanket and divertor. As in ARIES-ACT-1 [12], the thin VV (10 cm) of ARIES-ACT-2 is made of 3Cr-3WV bainitic steel [23], cooled with helium, and runs hot at ~300°C to avoid issues related to tritium accumulation. The primary shielding component (LT shield) is located outside the thin VV. This shield operates at room temperature to help dissipate the decay heat during loss of coolant/flow accidents. The highly efficient WC filler was excluded to help control the decay heat of the IB side during such accidents [24,25].

The ARIES-ACT-2 radial/vertical builds satisfy many criteria. The VV and magnets are lifetime components. The design requirements of Table II determine the combined dimensions of blanket and SR needed to protect the VV for 40 FPY life of plant. To enhance the power balance, an additional requirement was set to maximize the recoverable nuclear heating from the blanket and SR (~ 99% of the thermal power) and minimize the low-grade heat leaking to both VV and LT shield (~ 1% of the thermal power). This particular requirement mandates at least 30 cm thick SR. Another special requirement concerns shielding the 16 maintenance ports located on the OB side. A 45 cm thick He-cooled shielding plug placed at the inner radius of the maintenance ports helps protect the sides of the TF magnets.

A common goal for all specialized components (blanket, SR, and VV) is to provide a shielding function to collectively satisfy the radiation protection requirements for the superconducting (S/C) magnets. This helps define the most compact operational space of the machine with minimum radial standoff to free ex-vessel space for structural connections, cooling pipes, coil leads, etc. Using the PARTISN code [26] and FENDL-2.1 data library [16], 1-D tradeoff analyses of water and B-FS filler defined the optimal composition of IB, OB, and top/bottom LT shields with FS structure. Figure 12 displays the optimum radial/vertical builds based on ARIES-ACT-2 specifications while Table III lists the composition of all components.

It should be emphasized that the radial/vertical build defined thus far has been assumed to be free of penetrations. As anticipated, several penetrations for plasma heating and current drive exist around the OB midplane, protruding through all OB components. Such penetrations along with the 16 assembly gaps allow neutrons to stream through, putting the shield efficiency in jeopardy. Due to the limited scope of this study, only the effect of assembly gaps has been addressed for IB and OB components and the 3-D results will be published in a separate document.

Table II. ARIES-ACT-2 Design Requirements and Radiation Limits

| | |
|---|--|
| Calculated overall TBR (for T self-sufficiency) | 1.05 with ^6Li enrichment < 90% |
| Damage to structure (for structural integrity) | 200 dpa for advanced ferritic steel |
| Reweldability of RAFM steel (assumed) | 1 He appm |
| S/C magnets (@ 4 K): | |
| Peak fast n fluence to Nb_3Sn ($E_n > 0.1$ MeV) | 10^{19} n/cm 2 |
| Peak nuclear heating | 2 mW/cm 3 |
| Peak dpa to Cu stabilizer | 6×10^{-3} dpa |
| Peak dose to GFF polyimide insulator | 10^{11} rads |
| Plant lifetime | 40 full power years |
| Plant availability | 85% |
| Operational dose rate to workers and public | 2.5 mrem/h |
| Nuclear heat leakage to LT components | $\sim 1\%$ (low-grade heat) |

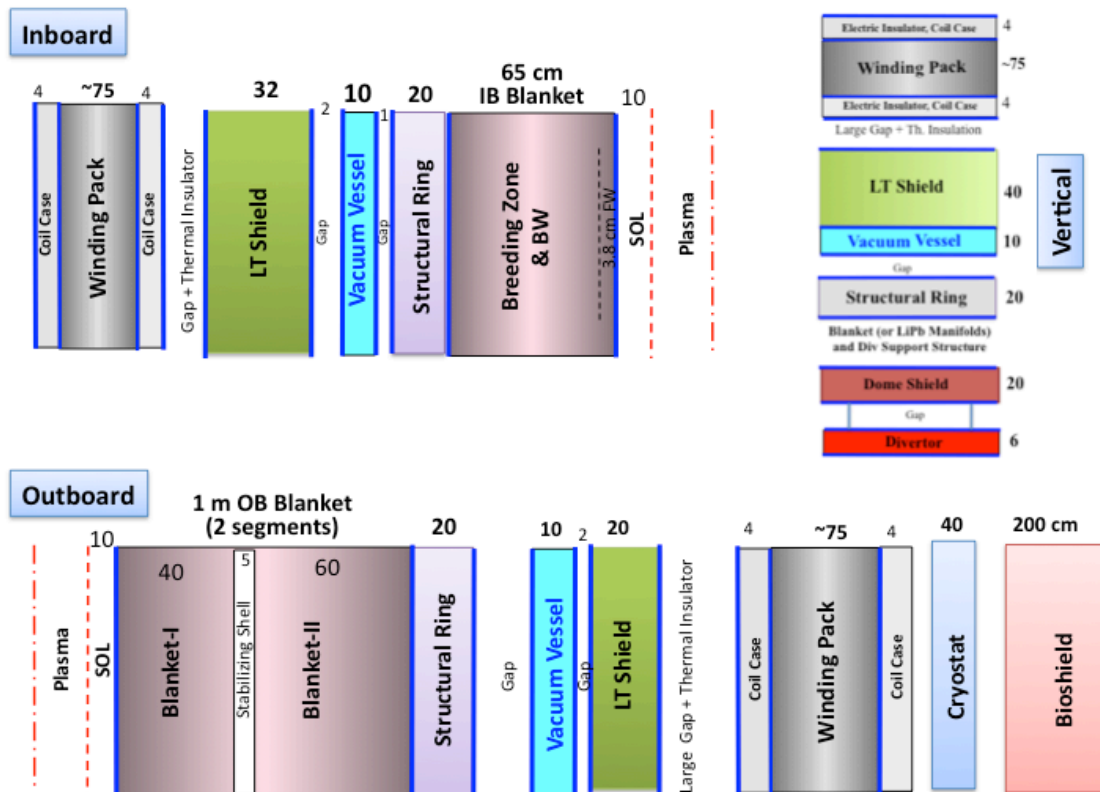


Fig. 12. ARIES-ACT-2 radial build at midplane and vertical build through divertor dome.

Table III. Composition of ARIES-ACT-2 Components (in vol%)

| | Inboard | Top/Bottom | Outboard |
|-----------------|--|--|--|
| FW/Blanket-I | 70.9% LiPb with 40% ⁶ Li enrichment, 10.8% FS, 5.5% SiC FCI, 12.8% He | 70.9% LiPb with 40% ⁶ Li enrichment, 10.8% FS, 5.5% SiC FCI, 12.8% He | 61.2% LiPb with 40% ⁶ Li enrichment, 15.4% FS, 7.1% SiC FCI, 16.3% He |
| Blanket-II | | | 73.0% LiPb with 40% ⁶ Li enrichment, 11.0% FS, 6% SiC FCI, 10.0% He |
| Divertor Plates | | 9% W armor, 36% W alloy, 11% ODS FS, 44% He | |
| LT Shield | 17% 3Cr-3WV FS, 39% H ₂ O, 44% B-FS | 15% 3Cr-3WV FS, 40% H ₂ O, 45% B-FS | 24% 3Cr-3WV FS, 44% H ₂ O, 32% B-FS |
| Shielding Plug | | | 22% 3Cr-3WV FS, 73% B-FS, 5% He |
| Structural Ring | | 80% FS, 20% He | |
| Vacuum Vessel | | 60% 3Cr-3WV FS, 40% He | |
| Coil Case | | 95% JK2LB steel, 5% LHe | |
| Winding Pack | 75% JK2LB steel, 12% Cu, 2% Nb ₃ Sn, 2.5% GFF polyimide insulator, 8.5% LHe | | |

VI. Nuclear Heating Profile

The 3-D TBR model shown in Fig. 4 has been used to evaluate the nuclear heating and overall energy multiplication using LiPb with 40% ⁶Li enrichment and fusion power of 2637.5 MW. Table IV provides the breakdown of heating by components for a 1/16th module producing 35.1 MW_{th} in IB, 102.6 MW_{th} in OB, and 8.1 MW_{th} in the upper or lower divertor region. This heating is needed to obtain details on the thermal hydraulic analysis and eventually the thermo-mechanical stresses the device is subjected to during operation. The total recoverable nuclear heating amounts to 2462.1 MW. Figure 13 displays a visual distribution of the nuclear heating in all regions. As Table V indicates, the IB, OB, and divertor regions generate 23%, 67%, and 10% of the heating, respectively. About 91% of the heating is deposited in the FW/blanket, stabilizing shells, and SR while the divertor and its support structure capture 9% of the heating. Dividing the total heating by the neutron power (2637.5 MW x 0.8), an overall energy multiplication of 1.167 is obtained.

The split of the nuclear heating between the He and LiPb high temperature coolants is provided in Table VI, yielding 3119 MW of useful thermal energy including the surface heating. This split between the He and LiPb loads is an essential parameter for the power conversion system and also for the ARIES Systems Code for the purpose of costing the He and LiPb heat transfer/transport system. Most of the divertor and blanket He and LiPb pumping powers (~90%) are recovered by the He and LiPb coolants as thermal power. The end result is 49:51 for the He:LiPb thermal power ratio.

About 49.3 MW (1.6% of the total 3119 MW thermal power) is deposited in the VV and LT shield. In the IB, 28.5 MW is gathered and in the OB 19.1 MW is found. The remainder (1.7 MW) rests in the upper and lower VV and LT shield. This heat deposited in the VV and LT shield could be dumped as low-grade heat or used for facility and hot water heating. Such a small percentage of low-grade heat is made possible because of the thicker, 65 cm, IB blanket, which limits the amount of heat to leave the main internal components. Admittedly, the thicker IB blanket results in an increase in the capital and replacement costs and higher field at the TF magnet, but this could be offset to a large extent by the higher output power. In the final design, the He manifolds are not embedded in the blanket as shown in Fig. 4. Rather, they are placed outside the IB blanket and OB blanket-I to help minimize the heat leakage.

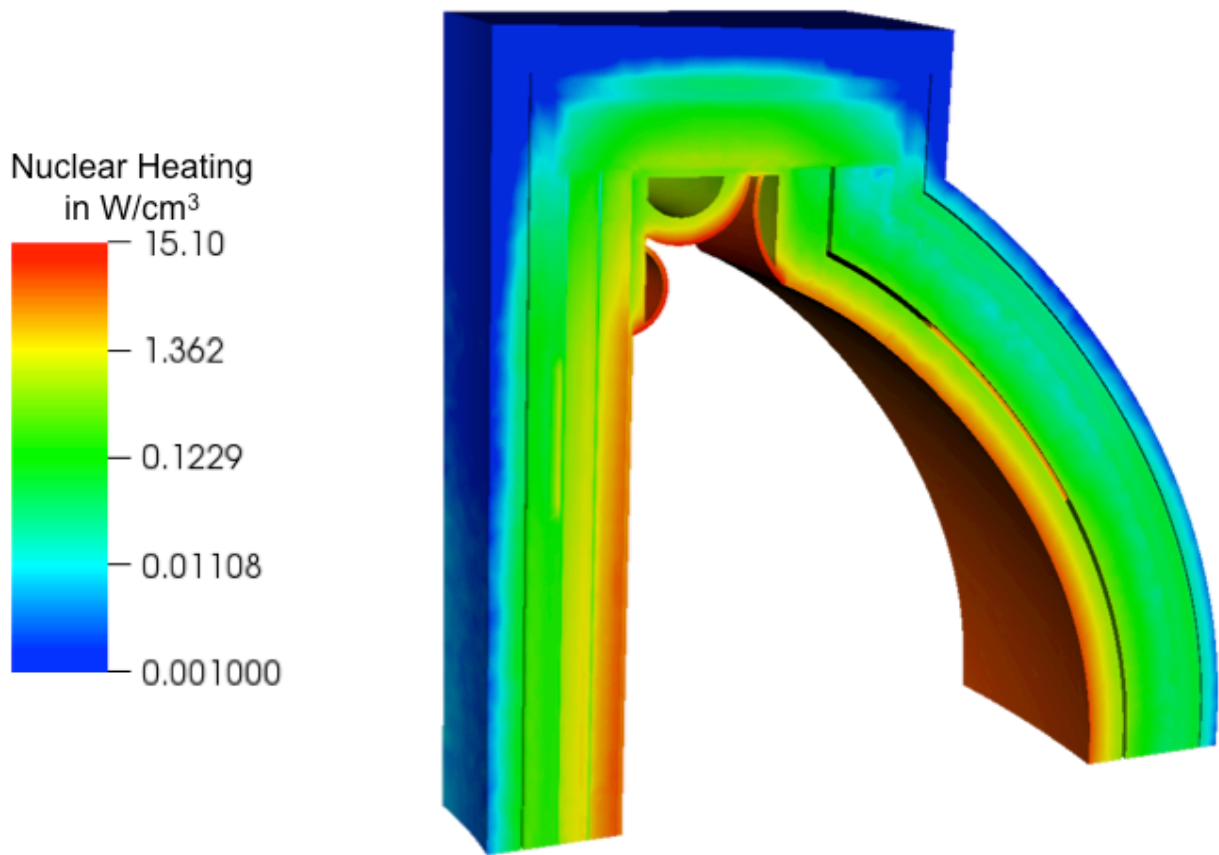


Fig. 13. Nuclear heating profile for ARIES-ACT-2 components.

Table IV. Detailed Breakdown of Nuclear Heating in 1/16th Module

| Inboard Nuclear Heating | MW |
|-----------------------------------|----------------|
| 65 cm Thick IB Blanket: | 33.148 |
| 3.8 cm FW | 3.081 |
| 58.2 cm Breeding Zone | 29.364 |
| LiPb Flow Channels | 27.507 |
| FS/He Cooling Channels | 0.900 |
| SiC Flow Channel Inserts (FCI) | 0.958 |
| 3 cm Back Wall | 0.298 |
| 3.8 cm Side Wall | 0.368 |
| IB Manifold | 0.037 |
| 4 cm VS Shell | 0.523 |
| IB Structural Ring | 1.449 |
| Total IB Heating | 35.119 |
| IB Vacuum Vessel | 1.261 |
| IB LT Shield | 0.517 |
| Outboard Nuclear Heating | |
| 40 cm Thick OB-I Blanket: | 78.854 |
| 3.8 cm FW | 8.654 |
| 33.2 cm Breeding Zone | 67.530 |
| LiPb Flow Channels | 60.685 |
| SiC FCI | 3.687 |
| FS/He Cooling Channels | 3.159 |
| 3 cm Back Wall | 1.824 |
| 3.8 cm Side and Top Wall | 0.623 |
| OB-I Manifold | 0.223 |
| 60 cm Thick OB-II Blanket: | 17.885 |
| 3 cm FW | 0.806 |
| 54 cm Breeding Zone | 16.778 |
| LiPb Flow Channels | 16.112 |
| SiC FCI | 0.334 |
| FS/He Cooling Channels | 0.332 |
| 3 cm Back Wall | 0.180 |
| 3.8 cm Side and Top Wall | 0.112 |
| OB-II Manifold | 0.009 |
| 4 cm VS Shell | 4.628 |
| OB Structural Ring | 1.248 |
| Total OB Heating | 102.615 |

| | |
|--|--------------|
| OB Vacuum Vessel | 0.877 |
| OB LT Shield | 0.323 |
| Divertor Nuclear Heating (MW) | |
| Upper or Lower Divertor: | |
| 6 cm W-based Divertor Plates: | 3.854 |
| Inner Plate | 1.166 |
| Dome Plate | 1.506 |
| Outer Plate | 1.182 |
| Dome Shield | 1.513 |
| Divertor Support Structure | 1.634 |
| Blanket/Manifolds | 1.009 |
| Structural Ring | 0.066 |
| Total Upper or Lower Divertor Heating | 8.076 |
| Upper/Lower Vacuum Vessel | 0.040 |
| Upper/Lower LT Shield | 0.012 |

Table V. Broad Breakdown of Nuclear Heating in ARIES-ACT-2 Components

| Nuclear Heating (MW): | Inboard | Outboard | Divertor | Total |
|---|----------------|-----------------|-----------------|---------------|
| FW/Blanket | 530.4 | 1547.8 | 32.3 | 2110.5 |
| Divertor Plates, Support Structure, Dome Shield | -- | -- | 224 | 224 |
| Stabilizing Shells | 8.4 | 74 | -- | 82.4 |
| Structural Ring | 23.1 | 20 | 2.1 | 45.2 |
| Total Recoverable Heat | 561.9 | 1641.8 | 258.4 | 2462.1 |
| Unrecoverable Heating (MW): | | | | |
| Vacuum Vessel | 20.2 | 14 | 1.3 | 35.5 |
| LT Shield | 8.3 | 5.1 | 0.4 | 13.8 |
| Total Low-Grade Heat | 28.5 | 19.1 | 1.7 | 49.3 |

Table VI. Thermal Power Split Between He and LiPb Coolants

| Thermal Power (MW_{th}) | He | LiPb | Total |
|--|-------------|-------------|---------------|
| Surface Heating | 633.4 | --- | 633.4 |
| Recovered Power from Divertor Pumping | 10.9 | --- | 10.9 |
| Recovered Power from Blanket Pumping | ~6 | ~6 | 12 |
| FW/Blankets, Manifolds, and Stabilizing Shells | 497.2 | 1696.2 | 2193.4 |
| | | | |
| Divertor Plates, Support Structure, Dome Shield | 224 | --- | 224 |
| Structural Ring | 45.2 | --- | 45.2 |
| Leakage from LiPb to He | ~+100 | ~-100 | 0 |
| Total | 1517 | 1602 | 3119 |
| | (~49%) | (~51%) | |

VII. Radiation Damage to Structural Components

ARIES-ACT-2 employs RAFM steels for the fusion power core and W alloys for the stabilizing shells and innermost layers of divertor plates. The service lifetimes of ARIES-ACT-2 components (FW/blanket, SR, VV, shield, and divertor) depend on the life-limiting criteria for these structural materials. Historically, the thermal and mechanical stresses, thermal creep, atomic displacement, and activation products have led to either a failure mechanism or a violation of the low-level waste requirement, therefore prematurely ending the service lifetime of structural components. For FS-based components, the life-limiting criterion has traditionally been the displacement of atoms. During the past 20 years of ARIES studies, we have adopted the limit of 200 displacements per atom (dpa) for advanced FS structure [5,7,12]. The life-limiting criterion for W alloys is unknown, so the divertor system is assumed to be replaced with the FW/blanket during the 40 FPY plant lifetime.

The recent development of materials for fusion applications delivered a class of low-activation, radiation-resistant ferritic/martensitic steels with low neutron-induced swelling. ARIES-ACT-2 employs F82H [27] for FS-based components. The peak dpa and He production occur at the midplane of the OB FW, reaching 21 dpa/FPY and 225 He appm/FPY, respectively, indicating He/dpa ratio of 10.7 and FW/blanket lifetime of 9.5 FPY.

There is a concern regarding the 14 MeV source neutrons streaming through the assembly gaps between modules and reaching the SR and VV producing excessive damage. A set of 3-D analyses is underway to evaluate the radiation damage to FS-based components in the presence of the IB and OB assembly gaps. There are 2 cm wide radial/poloidal assembly gaps separating the 16 toroidal modules. As the power core heats up, these gaps close partially. Also during operation, neutron-induced swelling will contribute to the gaps' width decreasing. As designers and operators become more experienced with the evolution of such gaps during plant operation, they will design the gap width properly to avoid any adverse interlocking or secondary stresses at contact points. For any gap width, the top, middle and bottom of the assembly gaps behave differently during operation due to the non-uniform structure temperature and NWL distribution. Because the evolution of gaps during operation in the three toroidal, poloidal, and radial directions is extremely complex and difficult to predict, the ongoing 3-D streaming analysis will examine the peak dpa and He production at IB and OB SR and VV for a maximum gap width of 2 cm.

The majority of past ARIES designs [1] employed the RAFM F82H steel [27] for FS-based components without paying much attention to the choice of FS alloy. This F82H FS has a composition specifically tailored to facilitate the near-surface waste disposal and/or recycling after plant decommissioning. However, during assembly of large components (such as the VV), F82H would normally require heat treatment at 700-750°C for 0.5 to 2 hours after welding to temper the martensitic structure and develop high toughness combined with a low ductile-to-brittle-transition-temperature (DBTT). The necessity to temper the F82H FS at 700-750°C presents some difficulty for large components. For this reason, F82H is unacceptable for the VV due to the complex heat treatment requirement. Selection of an austenitic stainless steel, such as 316-SS, would eliminate the DBTT issue as well as the need for welds to be tempered at 750°C. However, there are several activation and material-related issues that would not support such a choice [23,25]. Such issues and others require careful evaluation from the perspective of VV fabrication, materials properties under irradiation, and activation. Reference 23 presents a thorough evaluation of seven steel options considered for the VV. The main concerns are related to the fabrication of a sizable VV (welding, PWHT, etc.), properties under irradiation (DBTT

shift, corrosion resistance, swelling, etc.), and activation (recyclability, clearability, low-level or high-level waste). It appears from this study the newly developed 3Cr-3WV bainitic FS mitigates most of the identified F82H problems. Besides meeting the activation requirements, this steel has the potential to satisfy the fabrication requirements for ARIES-ACT VV. The 3Cr-3WV bainitic FS will also be used in the LT shield.

The preferred option for the SR is the more advanced oxide dispersion-strengthened (ODS) FS to recover the nuclear heating at high temperature ($\sim 700^{\circ}\text{C}$) and enhance the power balance [2]. However, based on past analyses [23,24], the safety analysis may suggest more advanced alloys for the inboard SR, VV, and LT shield to be able to reuse such components after reaching high temperatures (1000°C or more) during severe LOCA/LOFA accidents and avoid replacing them when exceeding the 750°C reusability limit for F82H FS. The high Cr nano-structured ferritic alloys (NFA) offer the most promising approach to the development of materials for such components.

VIII. Activation and Environmental Impact of ARIES-ACT-2

Fusion has long been envisioned as possessing an inherent advantage for benign environmental impact, mainly due to the absence of high-level waste (HLW) generation. However, fusion tends to generate a sizable amount of mildly radioactive materials. Such a potential problem has been overlooked in early fusion studies and/or relegated to the back-end as only a disposal issue in low-level waste (LLW) repositories, adopting the preferred radioactive waste (radwaste) management approach of the 1960s. To put matters into perspective, we compared in Fig. 14 the power core volumes of the ITER [3] experimental device, ARIES-ACT-1&2 [2], and the European Power Plant Conceptual Study (PPCS) [28] to ESBWR (Economic Simplified Boiling Water Reactor) – a Gen-III⁺ advanced fission reactor [29]. As noted, fusion power cores generate sizable volumes of mildly activated materials compared to fission. Figure 15 illustrates the volumes of components comprising the fusion core (FPC) of ARIES-ACT-2.

Surrounding the fusion power core is the bioshield (shown in Fig. 1) – a 2 m thick, steel-reinforced concrete building constructed to withstand natural phenomena and essentially protects the public and workers against radiation. Being away from the plasma, the bioshield is subject to low radiation and contains very low radioactivity. However, its volume (not included in Figs. 14 and 15) dominates the waste stream. Since burying such a huge volume of slightly activated materials in geologic repositories is impractical, regulatory agencies around the globe suggested the clearance concept where such components could temporarily be stored for the radioactivity to decay, then released to the commercial market for reuse as shielding blocks, concrete rubble base for roads, deep concrete foundations, non-water supply dams for flood control, etc.

In recent years, we paid much attention to the waste management issue associated with the large volume of radioactive materials discharged from fusion power plants. This has been accomplished by efforts in the US [30-33] and throughout the world [34-38]. Essential steps included reshaping the fusion waste management approach and maximizing the reuse of materials through recycling and clearance in order to reclaim valuable resources in the form of metal alloys and concrete rubble, minimize the environmental impact, free ample space in repositories, and, in the long run, save fusion millions of dollars for the high disposal cost.

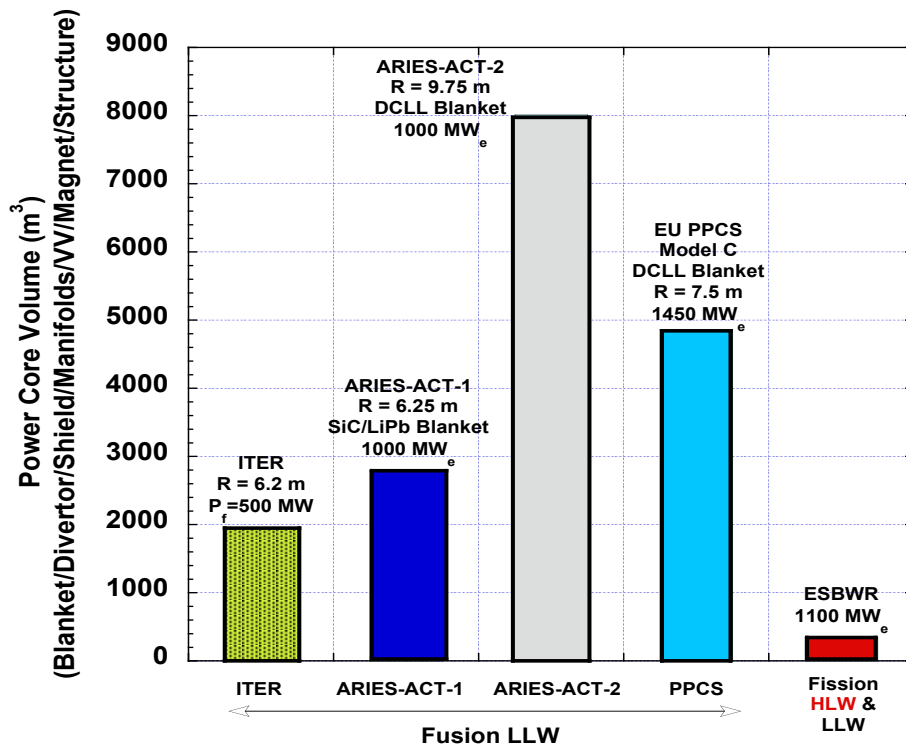


Fig. 14. Comparison of radwaste from power core of fusion and fission designs (actual volumes of components; not compacted; no replacement; no plasma chamber).

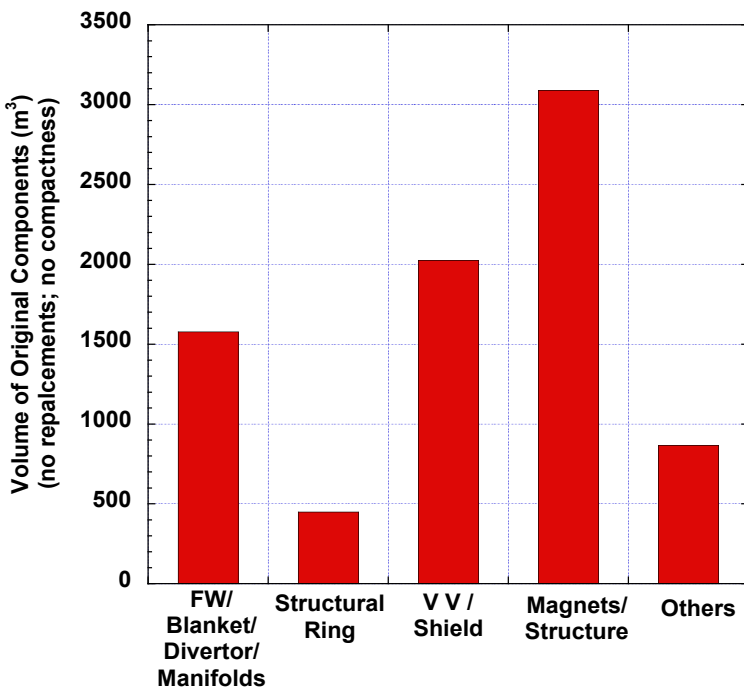


Fig. 15. Volumes of ARIES-ACT-2 FPC components.

This Section discusses the importance of handling the mildly radioactive materials produced in ARIES-ACT-2 power plant. We evaluated the disposal, recycling, and clearance approaches using the PARTISN radiation transport code [26], ALARA activation code [41], and the most recent FENDL3 activation library [42]. As well be discussed shortly, all components are recyclable with advanced remote handling equipment, but none of the IB and top/bottom components are clearable. Thus, we focused our attention on the OB region to identify the alloying elements and radioisotopes that hinder the clearance of hefty components (such as the VV, shield, and magnet) and the necessary design changes that assure the clearability of the bioshield – the largest component in any fusion design.

VIII-a. Geologic Disposal Issues and Needs

The ARIES-ACT-2 waste disposal rating (WDR) has been evaluated for fully compacted components using the waste disposal limits developed by Nuclear Regulatory Commission (NRC) 10CFR61 [39] and Fetter [40]. The NRC waste classification is based largely on radionuclides that are produced in fission reactors, hospitals, research laboratories, and food irradiation facilities. In the early 1990s, Fetter and others [40] performed analyses to determine the Class C specific activity limits for all long-lived radionuclides of interest to fusion using a methodology similar to that of 10CFR61 [39]. Although Fetter’s calculations carry no regulatory acceptance, they are useful because they include fusion-specific isotopes. All fusion components should meet both NRC and Fetter’s limits until the NRC develops official guidelines for fusion waste. Also, the WDR is evaluated at 100 y after shutdown, allowing the short-lived radionuclides to decay. A WDR < 1 means LLW and WDR > 1 means HLW.

Table VII provides the alloying elements and impurities found in F82H FS. The nominal 18-impurity list (that includes 3.3 wppm Nb and 21 wppm Mo) was measured at JAERI in Japan. For new steels, such as 3Cr-3WV, the F82H impurities and density are used since doing physical property measurements on new steels may be too far into the future. In an effort to reduce the long-term radioactivity, Klueh et al. [27] provided a list of the lowest 17 impurities (having 0.5 wppm Nb and 5 wppm Mo) that have ever been achieved in large-scale melting and fabrication practices of various steels. In other words, these are the lowest concentrations that have ever been achieved in large-scale melting and fabrication practices. They are not specific to any particular steel composition and should be achievable at *present* with a relatively modest effort and cost.

Table VII. Compositions of Low-Activation Materials with “Nominal” and “Present” Impurities (in weight %; * indicates weight part per million (wppm))

| Alloy | F82H with Nominal Impurities | W Alloy | F82H with Present Impurities | 3Cr_3WV_FS with Nominal Impurities | 3Cr_3WV_FS with Present Impurities |
|------------------------------|------------------------------|---------|------------------------------|------------------------------------|------------------------------------|
| Density (g/cm ³) | 7.89 | 19.35 | 7.89 | 7.89 | 7.89 |
| C | 0.1 | *6 | 0.1 | 0.1 | 0.1 |
| N | | *1 | | | |
| O | | *2 | | | |

| | | | | | |
|-----------|----------|--------|-----------|-----------|-----------|
| Na | | | | | |
| Al | 1.40E-03 | *1 | *30 | 1.40E-03 | *30 |
| Si | | *1 | | 0.14 | 0.14 |
| K | | *1 | | | |
| Sc | | | | | |
| V | 0.2 | | 0.2 | 0.25 | 0.25 |
| Cr | 7.5 | *3 | 7.5 | 3 | 3 |
| Mn | | | | 0.5 | 0.5 |
| Fe | 90.11586 | *8 | 90.173301 | 92.945858 | 93.003301 |
| Co | *28 | | *8 | *28 | *8 |
| Ni | *474 | *2 | *13 | *474 | *13 |
| Cu | *100 | *1 | *10 | *100 | *10 |
| Zn | | | | | |
| Ga | | | | | |
| As | | | | | |
| Se | | | | | |
| Br | | | | | |
| Rb | | | | | |
| Sr | | | | | |
| Zr | | | | | |
| Nb | *3.3 | | *0.5 | *3.3 | *0.5 |
| Mo | *21.0 | *12 | *5 | *21 | *5 |
| Pd | *0.05 | | *0.05 | *0.05 | *0.05 |
| Ag | *0.1 | | *0.05 | *0.1 | *0.05 |
| Cd | *0.4 | *1 | *0.05 | *0.4 | *0.05 |
| In | | | | | |
| Sn | | | | | |
| Sb | | | | | |
| Cs | | | | | |
| Ta | 0.02 | | 0.02 | | |
| W | 2 | 99.996 | 2 | 3 | 3 |
| Os | *0.05 | | *0.05 | *0.05 | *0.05 |
| Ir | *0.05 | | *0.05 | *0.05 | *0.05 |
| Pb | | *1 | | | |
| Bi | *0.02 | | *0.05 | *0.02 | *0.05 |
| Eu | *0.05 | | *0.02 | *0.05 | *0.02 |
| Tb | *0.02 | | *0.02 | *0.02 | *0.02 |
| Dy | *0.05 | | *0.05 | *0.05 | *0.05 |
| Ho | *0.05 | | *0.05 | *0.05 | *0.05 |
| Er | *0.05 | | *0.05 | *0.05 | *0.05 |
| U | *0.05 | | | | |

http://www.entegris.com/ProductLine_catPremiumGraphite_divSpecialtyMaterials_lineSiC.aspx.

The F82H FS of the blanket, SR, VV, and LT shield was first examined with “nominal” impurities and then reexamined with “present” impurities. Our results showed that the blanket and SR with F82H FS and “nominal” impurities generates HLW, which does not satisfy the ARIES requirement of generating only LLW. On the other hand, the controlled “present” impurity levels allow the blanket and SR to achieve the desired Class C LLW classification. This stresses again the need for strict control of the undesirable impurities (particularly Nb and Mo) that generate HLW. The remaining components qualify as Class C LLW even with “nominal” impurities as shown in Table VIII. The LT shield and magnets are less radioactive than the in-vessel components and qualify as Class A LLW – the least hazardous type of waste. Excluding the clearable components (cryostat and bioshield), ~40% of the ARIES-ACT-2 waste (blanket, SR, VV, and divertor) qualifies as Class C LLW. The dominant radioisotope at 100 y after shutdown is ⁹⁴Nb (from 0.5 wppm Nb impurity in F82H). The remaining ~60% (LT shield and magnet) would fall under the Class A LLW category.

Table VIII. WDR of selected outboard components with nominal and present impurities

| WDR | Lifetime (FPY) | Nominal Impurities | Present Impurities |
|--------------------------|-----------------------|---------------------------|---------------------------|
| FW/Inner Blanket Segment | 9.5 | 1.6 | 0.3 |
| Outer Blanket Segment | 40 | 2.4 | 0.4 |
| Structural Ring | 40 | 0.9 | 0.2 |
| Vacuum Vessel | 40 | 0.3 | |
| LT Shield | 40 | 0.05 | |
| Winding Pack | 40 | 0.07 | |
| Bioshield | 40 | << 1 | |

Several critical issues for the disposal option can be identified based on the assessment of disposal situation in the US. These are listed below along with specific needs for the fusion community:

Disposal issues:

- High disposal cost that continues to increase (for preparation, characterization, packaging, interim storage, transportation, licensing, and disposal)
- No commercial HLW repositories exist in the US
- Limited capacity of existing LLW repositories
- Political difficulty of siting new repositories limits their capacity
- Prediction of repository’s conditions for long time into future
- Radwaste burden for future generations.

Disposal needs:

- Revised activity limits for fusion radioisotopes issued by NRC
- Official guidelines by NRC for Greater Than Class C waste classification
- Large and low-cost interim storage facility
- Repositories designed for T-containing materials
- Reversible disposal process and retrievable waste (to gain public acceptance and ease licensing).

VIII-b. Recycling Issues and Needs

In this study, the technical feasibility of recycling is based on the dose rate to the remote handling (RH) equipment. Essentially, the dose determines the RH needs (hands-on, conventional, or advanced tools to handle the radioactive components) and the interim storage period necessary to meet the dose limit. Advanced RH equipment has been used in the nuclear industry, in hot cells and reprocessing plants, and in spent fuel facilities [43]. While the fission processes may have no direct relevance to fusion, their success gives confidence that advanced RH techniques could be developed to handle high doses ($> 10,000$ Sv/h) for the recycling of fusion materials. Beside the recycling dose, other important criteria include the decay heat level during reprocessing, recycling of tritium-containing materials, physical properties of recycled products, and economics of fabricating complex shapes remotely.

Figure 16 displays the recycling dose for selected OB components of ARIES-ACT-2. The variation with time of the recycling dose shows a strong location dependence. All in-vessel components can potentially be recycled within a year after shutdown with advanced RH equipment that can handle 10,000 Sv/h or more. The FW is an integral part of the blanket. However, it is shown in Fig. 16 as a separate component to provide the highest possible dose to RH equipment. The average FW/blanket dose is an order of magnitude lower. ^{54}Mn (from Fe) is the main contributor to the dose of FS-based components (FW, blanket, SR and VV) at early cooling periods (< 10 y), while impurities have no impact on the recycling dose during such a period. Storing the FW/blanket temporarily for several years helps drop the dose by a few orders of magnitude before recycling. The outermost components (cryostat and bioshield) contain very low radioactivity and can be recycled with hands-on following a specific cooling period. We do not expect significant dose build-up due to the reuse of materials after numerous life cycles based on previous multiuse analysis performed for the ARIES divertor [38].

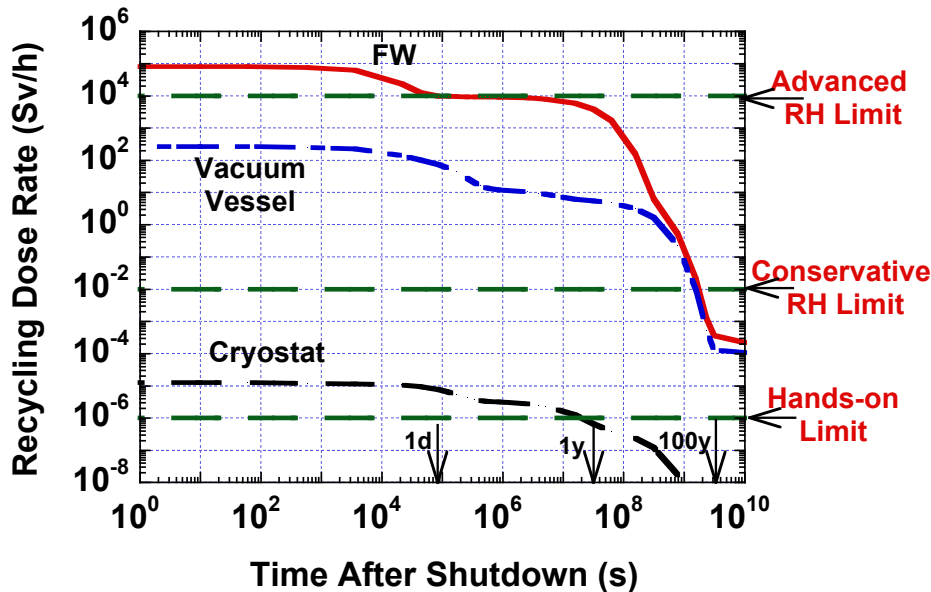


Fig. 16. Recycling dose rate to RH equipment for selected ARIES-ACT-2 OB components.

Since the recycling approach plays an essential role in minimizing the volume of radwaste, it should be pursued despite the lack of detail on how to implement it at the present time. Based on known areas involved in the recycling process, we identified several key issues for the fusion community to examine with a dedicated R&D program:

Recycling issues:

- Separation of various activated materials from complex components
- Radiochemical or isotopic separation processes for some materials, if needed
- Treatment and remote re-fabrication of radioactive materials
- Radiotoxicity and radioisotope buildup and release by subsequent reuse
- Properties of recycled materials? Any structural role? Reuse as filler?
- Inspection of parts made of recycled materials
- Handling of T containing materials during recycling
- Management of secondary waste. Any materials for disposal? Volume? Radwaste level?
- Energy demand for recycling process
- Cost of recycled materials
- Recycling plant capacity and support ratio.

Recycling needs:

- Radiation-resistant remote handling equipment
- Reversible assembling process of components and constituents (to ease separation of materials after use)
- Efficient detritiation system to remove tritium before recycling
- Large and low-cost interim storage facility with decay heat removal capacity
- Nuclear industry should accept recycled materials
- Recycling infrastructure.

VIII-c. Clearance Issues and Needs

The majority of nuclear waste (essentially the bioshield) contains traces of radioactive nuclides that represent no risk to the public safety and health. Over the past several decades, researchers in the nuclear field have attempted to issue policy statements to deregulate such materials with low concentrations of radioactive contamination. If this effort succeeds, the clearable materials will not be subject to regulatory control, be handled as if they are no longer radioactive, and be unrestrictedly recycled into consumer products (tables, chairs, tools, building and road materials, etc.). In 2003, the NRC declared materials with low concentrations of radioactivity can be deregulated and issued the NUREG-1640 documents [44] to obtain the clearance indices (CI) for the 115 radioisotopes that can be found in four types of clearable materials: steel, copper, and aluminum scrap, and concrete rubble. In 2004, the International Atomic Energy Agency (IAEA) published clearance standards [45] for 257 radionuclides, claiming to take into account the US NUREG-1640 evaluation [44].

Here, the NRC guidelines are referred to as the proposed US CI limits since the NRC has not yet issued an official policy on the unconditional release of materials. The CI for a clearable material is calculated as the ratio of the activity (in Bq/g) of the individual radioisotope to the allowable clearance limit summed over all radioisotopes. A material qualifies for clearance if the CI drops below one at any time during a defined storage period (< 100 y) following replacement or decommissioning. For components with multiple materials, it is essential to segregate and re-

evaluate the CIs for constituents. Sizable components, such as the 2 m thick bioshield, should be segmented into small layers with the CI for each layer reexamined.

For ARIES-ACT-2, the CIs for all internal components (blanket, SR, VV, LT shield) exceed unity by a wide margin even after an extended period of 100 y (refer to Fig. 17). Nb-94 (from Nb impurity) is the main contributor to the CI of FS-based materials at 100 y. A frequently asked question is: what material(s) or impurities deter the clearance of the VV (and LT shield)? It would be beneficial to clear such hefty components even after an extended storage of 100 y after shutdown. We examined the OB VV in detail and identified the major radioisotopes contributing to its 970 CI at 100 years. The main sources of these radioisotopes are the Nb, Eu, and Co impurities. Interestingly, an OB VV made of pure iron would have a CI of ~ 7 at 100 y (from Co-60 generated by Fe). This means no matter how serious an attempt is to strictly control all impurities or alter the alloying elements of the 3Cr-3WV steel, the VV (and LT shield) will never qualify for clearance, but remains recyclable, however. In other words, recycling is the only viable option to avoid disposing the FPC activated materials and to minimize the radwaste volume assigned for geologic repositories.

Even though the magnet is well protected by the blanket, VV and LT shield, not all constituents are clearable even after 100 years of storage. While the outer coil case is clearable shortly after shutdown, the inner coil case is not, as shown in Fig. 18. Examining the individual constituents of the winding pack (75% JK2LB steel structure, 12% Cu stabilizer, 2% Nb₃Sn conductor, 2.5% electric insulator, and 8.5% LHe, by volume) reveals that the CI of Nb₃Sn conductor is the dominant value and only the 12% Cu stabilizer could be cleared in less than 100 y (see Fig. 18).

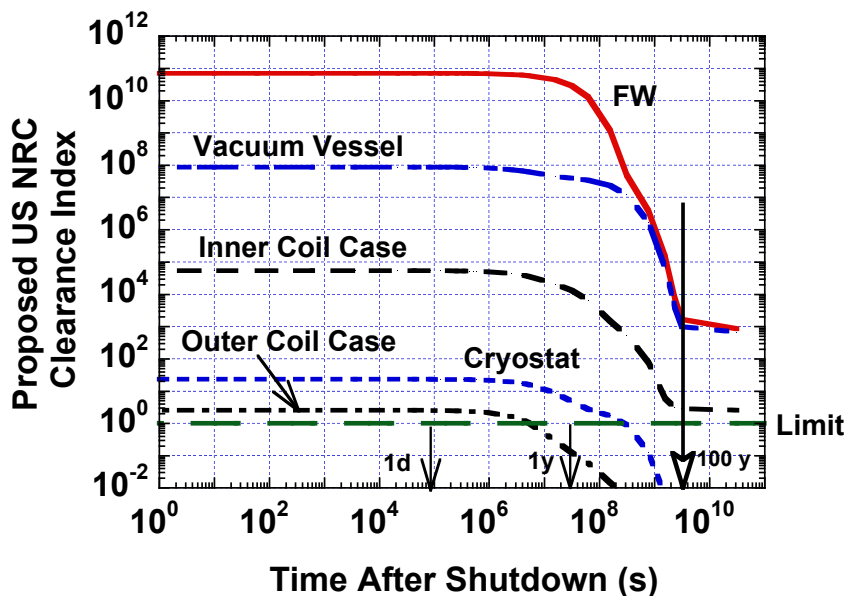


Fig. 17. Variation of CI with time after shutdown for selected ARIES-ACT-2 OB components.

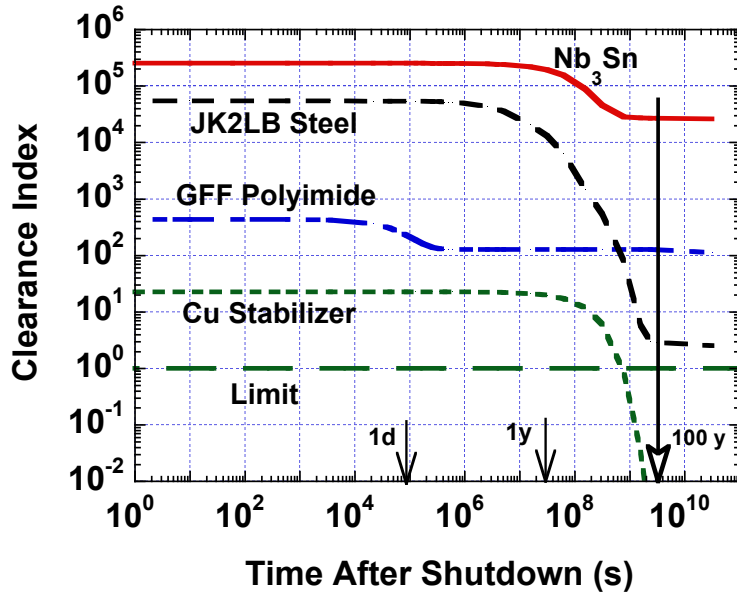


Fig. 18. Clearance indices of OB magnet constituents. CIs of Cu and steel evaluated with US NRC clearance limits while CIs of Nb₃Sn and GFF polyimide evaluated with IAEA clearance limits.

The 2 m thick external concrete building (bioshield) that surrounds the tokamak represents the largest single component of the decommissioned materials, as shown in Fig. 19. Fortunately, if adequately protected from streaming neutrons, the bioshield along with the 40 cm thick cryostat (20% F82H FS and 80% void) qualify for clearance, representing ~65% of the total volume of ARIES-ACT-2 radioactive materials.

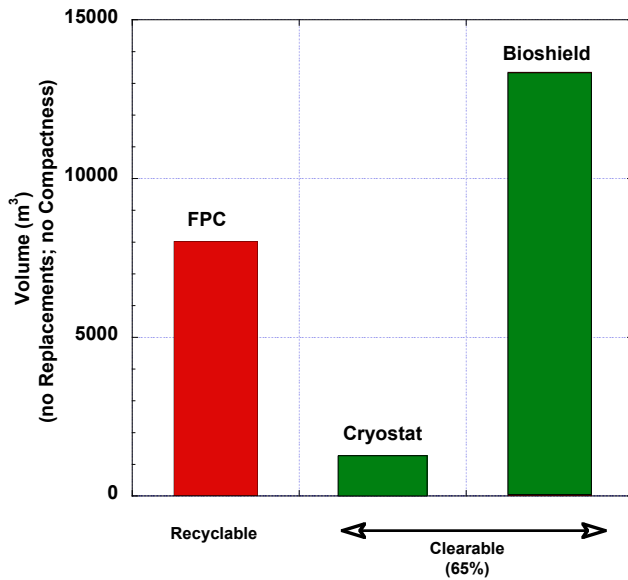


Fig. 19. Volumes of all ARIES-ACT-2 components: fusion power core, cryostat, and bioshield.

Special attention was paid to the variation of the neutron flux at the surface of the bioshield. Due to the presence of the 16 maintenance ports, the flux varies widely in the toroidal direction. The flux behind the outer leg of the TF magnet is 5×10^5 n/cm²s (refer to Fig. 20) while the flux behind the maintenance port is much higher (1×10^{11} n/cm²s). To reduce this flux to 5×10^5 n/cm²s (same level behind the magnet), ~30 cm thick local LT shield should be attached to the doors of the maintenance ports to attenuate the streaming neutrons during operation. We evaluated the CI for the bioshield constituents (85% Type-04 ordinary concrete, 10% mild steel, and 5% He by volume). Figure 21 shows the CI of the innermost surface layer (1 cm thick) of the bioshield. The concrete qualifies for clearance shortly after shutdown while the steel is clearable within a year. The outer layers exhibit much lower CI and both concrete and steel can be cleared immediately after decommissioning.

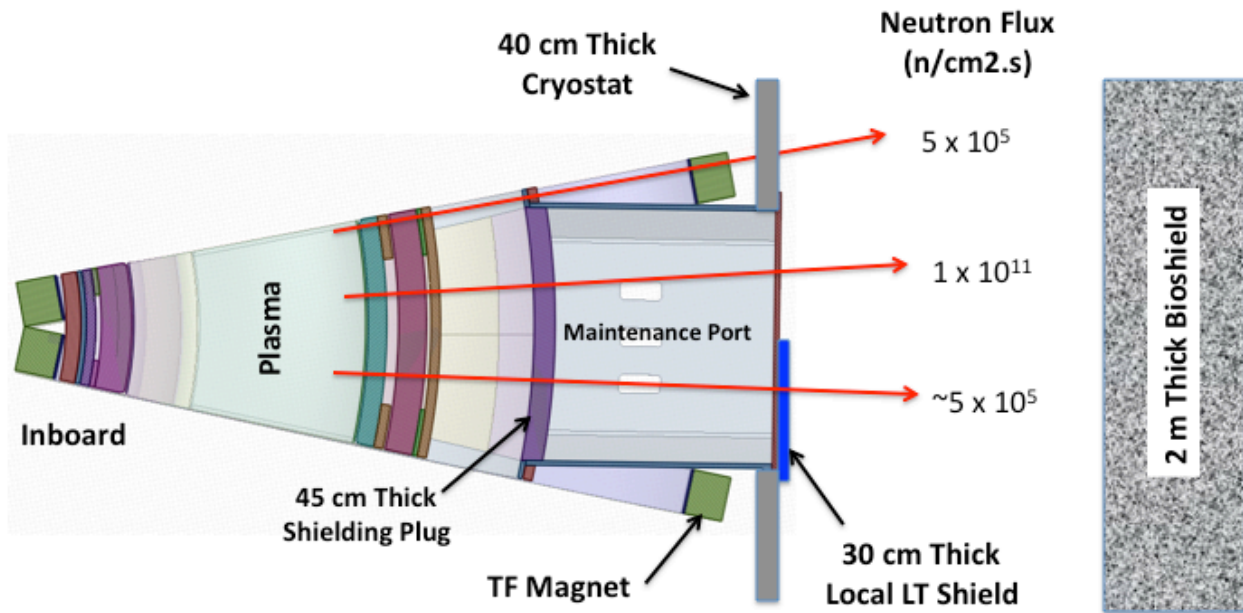


Fig. 20. Midplane view showing the neutron flux at various cross sections through ARIES-ACT-2 components.

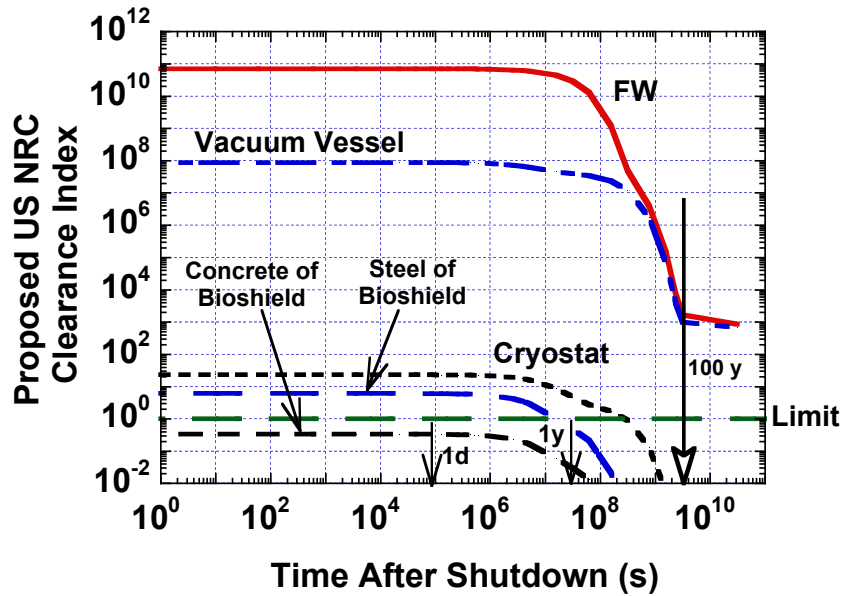


Fig. 21. Variation of bioshield CI with time after shutdown.

Our results indicate the ARIES-ACT-2 cryostat, bioshield, and some magnet constituents are clearable. It is unlikely that the missing fusion-related radioisotopes [46] from both US NRC and IAEA CI evaluations could alter our conclusions. Nevertheless, efforts by the US NRC, IAEA, and other organizations should continue to develop clearance standards for all radioisotopes of interest to fusion applications. We also support the national and international organizations' efforts to convince industrial as well as environmental groups that clearance of slightly radioactive solids can be conducted safely with no risk to the public health. Other clearance issues and needs that require further assessment include:

Clearance issues:

- Discrepancies between proposed US-NRC and IAEA clearance standards
- Impact on clearance index prediction of missing radioisotopes (such as ^{10}Be , ^{26}Al , ^{32}Si , $^{91,92}\text{Nb}$, ^{98}Tc , $^{113\text{m}}\text{Cd}$, $^{121\text{m}}\text{Sn}$, ^{150}Eu , $^{157,158}\text{Tb}$, $^{163,166\text{m}}\text{Ho}$, $^{178\text{n}}\text{Hf}$, $^{186\text{m},187}\text{Re}$, ^{193}Pt , $^{208,210\text{m},212}\text{Bi}$, and ^{209}Po)
- Radioisotope buildup and release by subsequent reuse.

Clearance needs:

- Official clearance limits issued by legal authorities
- Accurate measurements and reduction of impurities that deter clearance of in-vessel components
- Reversible assembly process of components and constituents
- Large and low-cost interim storage facility
- Clearance infrastructure
- Clearance market.

IX. Conclusions

In this report, we addressed the ARIES-ACT-2 nuclear system with high degree of accuracy. Some of the achievements include modeling the final design using the UW DAGMC code that has been able to tackle complex 3-D geometry by coupling the CAD system with the neutronics MCNP code. This coupling presents an invaluable tool to nuclear designers and helps gain much deeper understanding of the impact of the detailed geometry on the radiation environment.

Essential measures that helped deliver an optimal design include estimating the TBR with high fidelity, defining the radiation environment within the fusion power core in terms of accurate NWL profile, optimizing all components comprising the radial/vertical builds keeping in mind the activation characteristics of the preferred materials, and determining the nuclear heat loads to all components including the fine details of the blanket. Our results reveal that the ARIES-ACT-2 design satisfies the breeding requirements of 1.05 TBR with 40% ^6Li enrichment (< 90%), has an energy multiplication of 1.167, He:LiPb thermal power ratio of 49:51, and service lifetime of 9.5 FPY for the FW, blanket and divertor based on radiation damage considerations. Another important point is that the nuclear heating analysis proved to be of particular interest, calling for resizing the IB and OB components to enhance the power balance by limiting the unrecoverable low-grade heat deposited in VV and LT shield.

ARIES-ACT-2 is able to prevent generating HLW by employing low-activation materials with strict impurity control (e.g., < 1 wppm Nb). However, the amount of radioactive materials is large. Efforts to recycle and/or clear all ARIES-ACT-2 materials are necessary. Fortunately, the sizable bioshield along with the cryostat qualifies for clearance, representing ~65% of the total volume of ARIES-ACT-2 radioactive materials. Adequate protection against streaming neutrons is an essential requirement for the survivability of external components and to assure the clearability of the bioshield.

The desire to reclaim valuable resources in the form of metal alloys and concrete rubble persists in all industries, not only nuclear. To make the recycling and clearance approaches a reality, major rethinking, education, and research should be developed and pursued in the nuclear field. In the meantime, the fusion program should be set up to accommodate the recycling/clearance strategy to continue holding the promise of fusion energy production with low environmental impact.

Acknowledgment

This work was performed under the auspices of the US Department of Energy under contract #DE-FG02-98ER 54462.

References

1. The ARIES Project: <http://aries.ucsd.edu/ARIES/>.
2. C. KESSEL M. S. TILLACK, F. NAJMABADI et al., “The ARIES Advanced and Conservative Tokamak (ACT) Power Plant Study,” Fusion Science and Technology, 67, No. 1, 1-21 (Jan 2015).
3. The ITER Project: <http://www.iter.org/>.
4. F. NAJMABADI, The ARIES Team, “Spherical Tours Concept as Power Plants—the ARIES-ST Study,” Fusion Engineering and Design, 65, 143-164 (2003).
5. L. A. EL-GUEBALY, The ARIES Team, “ARIES-ST Nuclear Analysis and Shield Design,” Fusion Engineering and Design, 65, 263-284 (2003).

6. F. NAJMABADI, A. R. RAFFRAY and The ARIES-CS Team, "The ARIES-CS Compact Stellarator Fusion Power Plant," *Fusion Science and Technology*, 54, No. 3, 655-672 (2008).
7. L. EL-GUEBALY, P. WILSON, D. HENDERSON, M. SAWAN, G. SVIATOSLAVSKY, T. TAUTGES et al., "Designing ARIES-CS Compact Radial Build and Nuclear System: Neutronics, Shielding, and Activation," *Fusion Science and Technology*, 54, No. 3, 747 (2008).
8. M. WANG, D. HENDERSON, T. TAUTGES, L. EL-GUEBALY, and X. WANG, "Three-Dimensional Modeling of Complex Fusion Devices Using CAD-MCNP Interface," *Fusion Science and Technology*, 47, No. 4, 1079 (2005).
9. P. P. H. WILSON, R. FEDER, U. FISCHER, M. LOUGHLIN, L. PETRIZZI, Y. WU, and M. YOUSSEF, "State-of-the-Art 3-D Radiation Transport Methods for Fusion Energy Systems," *Fusion Engineering and Design*, 83, 824 (2008).
10. M. E. SAWAN, P. P. H. WILSON, T. TAUTGES, L. A. EL-GUEBALY, D. L. HENDERSON, T. D. BOHM, E. P. MARRIOTT, B. KIEDROWSKI, B. SMITH, A. IBRAHIM, and R. SLAYBAUGH, "Application of CAD-Neutronics Coupling to Geometrically Complex Fusion Systems," *Proceedings of 23rd IEEE/NPSS Symposium on Fusion Engineering (SOFE)*, May 31-June 5, 2009, San Diego, CA, ISBN No. 978-1-4244-2636-2, IEEE Cat. No. CFP09SOF-CDR.
11. P. P. H. WILSON, T. J. TAUTGES, J. A. KRAFTCHECK, B. M. SMITH, and D. L. HENDERSON, "Acceleration Techniques for the Direct Use of CAD-Based Geometry in Fusion Neutronics," *Fusion Engineering and Design*, 85, Issues 10-12, 1759 (2010).
12. L. EL-GUEBALY and L. MYNSBERGE, "Neutronics Characteristics and Shielding System for ARIES-ACT-1 Power Plant," *Fusion Science and Technology*, 67, No. 1, 107-124 (Jan 2015).
13. MCNP X-5 MONTE CARLO TEAM, "MCNP—A General Monte Carlo N-Particle Transport Code, Version 5." Volume I: Overview and Theory, LA-UR-03-1987; Volume II: User's Guide, LA-CP-03-0245; Volume III: Developer's Guide, LA-CP-03-0284, Los Alamos National Laboratory (October 2005).
14. "DAGMC Users Guide," University of Wisconsin-Madison Fusion Technology Institute (2008); <https://trac.cae.wisc.edu/trac/svalinn/wiki/DAGMCUsersGuide>.
15. "CUBIT Geometry and Mesh Generation Toolkit Version 12.2." Sandia National Laboratories, 2010; <http://cubit.sandia.gov>.
16. D. L. ALDAMA and A. TRKOV, "FENDL-2.1 Update of an Evaluated Nuclear Data Library for Fusion Applications," *International Atomic Agency Report INDC(NDC)-467* (2004).
17. L. EL-GUEBALY, A. JABER, and S. MALANG, "State-of-the-Art 3-D Assessment of Elements Degrading the TBR of the ARIES DCLL Blanket," *Fusion Science and Technology*, 61, 321 (2012).
18. L. EL-GUEBALY and S. MALANG, "Toward the Ultimate Goal of Tritium Self-Sufficiency: Technical Issues and Requirements Imposed on ARIES Advanced Fusion Power Plants," *Fusion Engineering and Design*, 84, 2072 (2009).
19. P. BATISTONI, M. ANGELONE, U. FISCHER, A. KLIX, I. KODELI, D. LEICHTLE, M. PILLON, W. POHORECKI, and R. VILLARI, "Tritium Breeding Experiments on HCPB and HCLL Blanket Mock-ups Irradiated with 14 MeV Neutrons," *Nuclear Fusion* 52, #8, 083014 (2012).

20. L. A. EL-GUEBALY and S. MALANG, "Need for Online Adjustment of Tritium Bred in Blanket and Implications for ARIES Power Plants," University of Wisconsin Fusion Technology Institute Report, UWFD-1372 (2009). Available at: <http://fti.neep.wisc.edu/pdf/fdm1372.pdf>.
21. P. HUBBERSTEY, T. SAMPLE, and M. BARKER, "Is Pb-17Li Really the Eutectic Alloy? A Redetermination of the Lead-Rich Section of the Pb-Li Phase Diagram ($0.0 < x_{\text{Li}}(\text{at}\%) < 22.1$)," *Journal of Nuclear Materials*, 191-194, 283 (1992).
22. C. KOEHLI, X. R. WANG, M. S. TILLACK and F. NAJMABADI, "Alternative Design Options for a Dual-Cooled Liquid Metal Blanket for ARIES-ACT2," UCSD Report, UCSD-CER-13-02, (2013); <http://aries.ucsd.edu/LIB/REPORT/ARIES-ACT/UCSD-CER-13-02.pdf>.
23. L. EL-GUEBALY, T. HUH, A. ROWCLIFFE, S. MALANG, and the ARIES-ACT Team, "Design Challenges and Activation Concerns for ARIES Vacuum Vessel," *Fusion Science and Technology*, 61, 449 (2013).
24. C. MARTIN and L. EL-GUEBALY, "ARIES-ACT-1 Loss of Coolant/Flow Accident Thermal Analysis," University of Wisconsin Fusion Technology Institute Report, UWFD-1416 (2013); <http://fti.neep.wisc.edu/pdf/fdm1416.pdf>.
25. L. EL-GUEBALY, L. MYNSBERGE, C. MARTIN, and D. HENDERSON, "Activation and Environmental Aspects of ARIES-ACT-1 Power Plant," *Fusion Science and Technology* 67, No. 1, 179-192 (Jan 2015).
26. R. E. ALCOUFFE, R. S. BAKER, J. A. DAHL et al., "PARTISN: A Time-Dependent, Parallel Neutral Particle Transport Code System," LANL Report, LA-UR-05-3925 (2005).
27. R. KLUEH, E. CHENG, M. L. GROSSBECK, and E. E. BLOOM, "Impurity Effects on Reduced-activation Ferritic Steels Developed for Fusion Applications," *Journal of Nuclear Materials*, 280, 353 (2000).
28. D. MAISONNIER, I. COOK, P. SARDAIN, R. AANDREANI, L. DI PACE, R. FORREST et al., "A conceptual study of commercial fusion power plants." Final Report of the European Fusion Power Plant Conceptual Study (PPCS), Report EFDA-RP-RE-5.0 (2005).
29. The ESBWR Design: http://www.gepower.com/prod_serv/products/nuclear_energy/en/new_reactors/esbwr.htm.
30. L. EL-GUEBALY, "Evaluation of Disposal, Recycling, and Clearance Scenarios for Managing ARIES Radwaste after Plant Decommissioning," *Nuclear Fusion*, 47, 485 (2007).
31. L. EL-GUEBALY, V. MASSAUT, K. TOBITA, and L. CADWALLADER, "Goals, Challenges, and Successes of Managing Fusion Active Materials," *Fusion Engineering and Design* 83, Issues 7-9, 928-935 (2008).
32. L. A. EL-GUEBALY, "Future Trend Toward the Ultimate Goal of Radwaste-Free Fusion: Feasibility of Recycling/Clearance, Avoiding Geological Disposal." *Journal of Plasma and Fusion Research*, 8, 3404041-1-6 (2013).
33. L. A. EL-GUEBALY and L. CADWALLADER, "Perspectives of Managing Fusion Radioactive Materials: Technical Challenges, Environmental Impact, and US Policy." Chapter in book: *Radioactive Waste: Sources, Management and Health Risks*. Susanna Fenton Editor. NOVA Science Publishers, Inc.: Hauppauge, New York, USA. ISBN: 978-1-63321-731-7 (2014).
https://www.novapublishers.com/catalog/product_info.php?products_id=51057.

34. V. MASSAUT, R. BESTWICK, K. BRODÉN, L. DI PACE, L. OOMS, and R. PAMPIN, State of The Art of Fusion Material Recycling and Remaining Issues, *Fusion Engineering and Design*, **82**, 2844-2849 (2007).
35. M. ZUCCHETTI, L. EL-GUEBALY, R. FORREST, T. MARSHALL, N. TAYLOR, and K. TOBITA, "The feasibility of Recycling and Clearance of Active Materials from a Fusion Power Plant," *Journal of Nuclear Materials*, **367-370**, 1355-1360 (2007).
36. M. ZUCCHETTI, L. DI PACE, L. EL-GUEBALY, B. N. KOLBASOV, V. MASSAUT, R. PAMPIN, and P. WILSON, "The Back End of the Fusion Materials Cycle," *Fusion Science and Technology*, **52**, No. 2, 109 (2009).
37. LUIGI DI PACE, LAILA EL-GUEBALY, BORIS KOLBASOV, VINCENT MASSAUT, and MASSIMO ZUCCHETTI, "Radioactive Waste Management of Fusion Power Plants," Chapter 14 in Book: *Radioactive Waste*. Dr. Rehab Abdel Rahman (Ed.), ISBN: 978-953-51-0551-0, InTech (April 2012). Available at <http://www.intechopen.com/books/radioactive-waste/radioactive-waste-management-of-fusion-power-plants>.
38. BORIS KOLBASOV, LAILA EL-GUEBALY, VLADIMIR KHRIPUNOV, YOUJI SOMEYA, KENJI TOBITA, and MASSIMO ZUCCHETTI, "Some Technological Problems of Fusion Materials Management," *Fusion Engineering and Design*, **89**, 2013 (2014).
39. US Code of Federal Regulations, Title 10, Energy, Part 61, Licensing Requirements for Land Disposal of Radioactive Waste, Section 55, Waste classification, US Government Printing Office, January 2014.
40. S. FETTER, E.T. CHENG, and F.M. MANN, "Long Term Radioactive Waste from Fusion Reactors: Part II," *Fusion Engineering and Design*, **13**, 239-246 (1990).
41. P. WILSON and D. HENDERSON, "ALARA: Analytic and Laplacian Adaptive Radioactivity Analysis: A Complete Package for Analysis of Induced Activation," University of Wisconsin Fusion Technology Institute Report. Volume I - UWFDI-1070. Volume II - UWFDI-1071 (1998).
42. FENDL3 Activation Library: <https://www-nds.iaea.org/fendl3/000pages/StarterLib/2011-12-01/>.
43. P. DESBATS, H. TOUBON, and G. PIOLAIN, "Status of Development of Remote Technologies Applied to Cogema Spent Fuel Management Facilities in France," ANS 10th International Topical Meeting on Robotics and Remote Systems for Hazardous Environments, Gainesville, Florida (2004).
44. R. ANIGSTEIN et al., "Radiological assessments for clearance of materials from nuclear facilities," volume 1, NUREG-1640, US Nuclear Regulatory Commission, June 2003. Available at: <http://www.nrc.gov/reading-rm/doc-collections/nuregs/staff/sr1640/>.
45. International Atomic Energy Agency, "Application of the concepts of exclusion, exemption and clearance," IAEA Safety Standards Series, No. RS-G-1.7 (2004). Available at: http://www-pub.iaea.org/MTCD/publications/PDF/Pub1202_web.pdf.
46. L. EL-GUEBALY, P. WILSON, and D. PAIGE, "Evolution of Clearance Standards and Implications for Radwaste Management of Fusion Power Plants," *Fusion Science and Technology*, **49**, 62 (2006).